# INVESTIGATION OF $m^6A$ AND $m^1A$ RNA METHYLATIONS IN TRIPLE NEGATIVE BREAST CANCER CELLS

**A Thesis Submitted to**
**the Graduate School of**
**İzmir Institute of Technology**
**in Partial Fulfillment of the Requirements for the Degree of**

**MASTER OF SCIENCE**

**in Molecular Biology and Genetics**

**by**
**Buket SAĞLAM**

**July 2024**
**İZMİR**

We approve this thesis of **Buket SAĞLAM**

**Examining Committee Members:**

**Prof. Dr. Bünyamin AKGÜL**
Molecular Biology and Genetics,
İzmir Institute of Technology

**Prof. Dr. Özden YALÇIN-ÖZUYSAL**
Molecular Biology and Genetics,
İzmir Institute of Technology

**Assist. Prof. Dr. Yavuz OKTAY**
Basic Medical Sciences,
Dokuz Eylül University

**12 July 2024**

**Prof. Dr. Bünyamin AKGÜL**
Molecular Biology and Genetics,
İzmir Institute of Technology

**Prof. Dr. Özden YALÇIN-ÖZUYSAL**
Head of the Department of
Molecular Biology and Genetics

**Prof. Dr. Mehtap Eanes**
Dean of Graduate School

# ACKNOWLEDGEMENTS

First of all, I would like to especially thank my supervisor Prof. Dr. Bünyamin AKGÜL for his support, guidance, comments and encouragement, and for being with me every step of the way and believing in me. I would like to express my gratitude and regards to TUBİTAK (Scientific and Technological Research Council of Turkey) for financially supporting me during my master's degree with BIDEB (Science Fellowships and Grant Programs) 2210-A Master's Scholarship Programs. I want to indicate my thanks and regards to Scientific Research Projects Coordinator Unit of İYTE due to their support and fund (Project No: 2022İYTE-2-0048).

I would like to indicate my special thanks to my committee members Prof. Dr. Özden YALÇIN-ÖZUYSAL and Asst. Prof. Dr. Yavuz OKTAY for their valuable time and comments to support my thesis.

I am also deeply thankful to Dr. İpek ERDOĞAN-VATANSEVER, Özge TÜNCEL and Seda BAYKAL for their valuable technical support, friendship, patience, and guidance. I extend my gratitude to my other colleagues, Azime AKÇAÖZ-ALASAR, Emine Beyza DOĞAN, Yasemin GAZALOĞLU, Zeynep Buse ORHAN, Dilek Cansu GÜRER, Ayşe Bengisu GELMEZ, Şirin Elife CEREN, and Yusuf Cem ÇİFTÇİ for their help in dealing with experiments. I cannot thank enough to my students Ahmet Batuhan DONDURUR and Ekin YILDIZ for their interests, helps, and friendships. I am also thankful to Biotechnology and Bioengineering Central Research specialists Özgür OKUR for her sincere help and kindness during my studies.

Special thanks should be given to Merve KARA, Melis ATBİNEK, and Özberk ŞEN for their support, motivation, and faith during my graduate life. My deepest thanks go to my family for their support and love during all of my all problems.

# ABSTRACT

## INVESTIGATION OF $m^6A$ AND $m^1A$ RNA METHYLATIONS IN TRIPLE NEGATIVE BREAST CANCER CELLS

Breast cancer is the most common type of cancer in women worldwide and divided into two sub-groups: invasive lobular and invasive ductal carcinoma. Invasive ductal carcinoma accounts for 80% of breast cancers. Triple negative breast cancer (TNBC) is also an aggressive type of breast cancer that fail to amplify estrogen receptor, progesterone receptor and human epidermal growth factor receptor 2. Intercalarily, RNA methylations have proven their effects on cell fate, especially in cancer studies. $m^6A$ and $m^1A$ have dynamic regulation mechanisms catalyzed by writer, reader and eraser proteins. These proteins have different expression levels based on cancer types and intended to be used for therapeutic/diagnostic approaches. In the current thesis study, it was aimed to examine the effects and comparison of $m^6A$ and $m^1A$ methylations in TNBC cell line, HCC1143, after METTL3 or TRMT61A silencing. Firstly, the maximum level of reduction in methylation amounts was attained at 72-hour as 41.2% decrease in $m^6A$ amount. To examine the phenotypic effects of silencing, we performed viability experiments and observed 40.1% and 27.4% decrease by METTL3 and TRMT61A knock-down, respectively. Additionally, G2/M phase arrest was observed upon METTL3 silencing. RNA sequencing experiments were conducted to evaluate the effects of knock-down at the molecular level. 585 differentially expressed genes (DEGs) were detected after reduction in $m^6A$ and 687 DEGs after TRMT61A silencing. 151 DEGs were common. Based on GO analyses, cell migration pathways were intensely observed in METTL3 while variability was observed in the immune-related and negative regulation of proliferation pathways after TRMT61A knock-down.

**Keywords:** *Triple negative breast cancer, $m^1A$ and $m^6A$ RNA modification, HCC1143, Viability, G2/M phase arrest*

# ÖZET

## ÜÇLÜ NEGATİF MEME KANSERİ HÜCRELERİNDE $m^6A$ VE $m^1A$ RNA METİLASYONLARININ ARAŞTIRILMASI

Meme kanseri dünya çapında kadınlarda en sık görülen kanser türüdür ve iki alt gruba ayrılır: invaziv lobuler ve invaziv duktal meme kanseri. Bunlardan invaziv duktal meme kanseri, %80 oranında dünya çapındaki meme kanserleri arasında yerini almaktadır. Üçlü negatif meme kanseri ise östrojen reseptörü, progesteron reseptörü ve insan epidermal büyüme faktörü reseptör 2'nin çoğaltılmasını gerçekleştiremeyen agresif bir meme kanseri alt türüdür. Kanser çalışmalarında RNA metilasyonları da hücrenin kaderine etkilerini kanıtlamış önde gelen modifikasyonlardır. Bütün metilasyonlarda olduğu gibi, $m^6A$ ve $m^1A$ de yazıcı, okuyucu ve silici proteinlerin yardımı ile gerçekleştirilen dinamik bir düzenleme mekanizmasına sahiptir. Bu proteinler, kanser türlerine göre farklı ifadelenme seviyelerine sahiptirler. Bu karakteristik özellikleri ile tedavi ve tespit amaçlı kullanılmaları hedeflenmektedir. Mevcut tez çalışmasında, yazıcı proteinleri olan METTL3 ve TRMT61A proteinlerinin susturulması sonrası, $m^6A$ ve $m^1A$ metilasyonlarının etkilerinin ve karşılaştırılmasının üçlü negatif meme kanseri hücrelerinden biri olan HCC1143 hücre hattında incelenmesi amaçlanmıştır. Öncelikle, METTL3 susturulması sonrası 72 saatte, maksimum düzey olan %41,2 oranında $m^6A$ miktarında azalma gözlenmiştir. Ardından fenotipik etkileri incelemek amaçlı gerçekleştirilen canlılık deneylerinde, METTL3 ve TRMT61A'nın susturulması ile sırasıyla %40,1 ve %27,4 azalma gözlemlendi. Ek olarak, TRMT61A'nın yıkılmasının aksine, yalnızca $m^6A$ metilasyonunun azalması sonucu G2/M fazında duraksama gözlenmiştir. $m^6A$ miktarının azaltılması sonucu 585 artan/azalan gen ve $m^1A$ metilasyonun azaltılması sonucu 687 artan/azalan gen tespit edilmiştir. Bunlardan 151 gen ortak olarak değişkenlik göstermiştir. Gen Ontolojisi zenginleştirme analizleri sonucunda METTL3 yıkımında hücre migrasyonu ve hücre motilite yolakları yoğun olarak gözlenmiştir. $m^1A$ azalması sonucu ise bağışıklık sistemi ve canlılığı negatif yönde etkileyen yolaklarda değişkenlik gözlenmiştir.

**Anahtar Kelimeler:** *Üçlü negatif meme kanseri, $m^1A$ ve $m^6A$ RNA modifikasyonu, HCC1143, Canlılık, G2/M fazı duraksaması*

# TABLE OF CONTENTS

# LIST OF FIGURES

**Figures** **Pages**

# LIST OF TABLES

**Tables** **Pages**

# CHAPTER 1

# INTRODUCTION

Epitranscriptomics, is a research area that focuses on biochemical modifications on ribonucleic acids (RNAs). These types of modifications including methylation, acetylation, uridylation and RNA editing of pseudouridine (Ψ) and adenosine-to-inosine (A-to-I) modulate RNA stability, structure, translation and regulation of non-coding RNAs (ncRNAs). Such modifications affect the cell fate in various types of diseases and disorders such as cancer. The occurrence of these modifications can be reversible based on the type and stage of cancer. Therefore, it is necessary to investigate the various modifications according to the type and severity of the disease. The profile that is examined differently can be helpful in the diagnosis of the cancer type or can be exploited as a therapeutic potential.

## 1.1. Breast cancer

Breast cancer is the most common cancer types in women worldwide and its diagnosis and treatment process vary according to histological and molecular subtypes (Harbeck et al. 2019). Breast cancer is histologically classified into two classes as invasive ductal carcinoma (IDC) and invasive lobular carcinoma (ILC). If it is classified as invasive, it means that the cancer cells can spread to surrounding tissues. While ILC starts in the glands of breast, IDC begins in the milk ducts that carry milk and is the most common breast cancer type accounting for nearly 80% of all breast cancers. ILC and IDC can also be divided into four subgroups based on the molecular basis: Luminal A, Luminal B, HER2 (human epidermal growth factor receptor 2) positive and triple negative, based on the expression of estrogen receptor (ER), progesterone receptor (PR) and HER2 receptor (Figure 1.1). (Di Leone et al. 2021; Harbeck et al. 2019). While Luminal A breast cancer subtype is ER/PR-positive, luminal B type breast cancer has lower ER/PR levels and can be HER2 receptor positive or negative. ER/PR-negative breast cancer mostly includes basal types and can be HER2-positive or HER2 negative. Triple-negative breast cancers (TNBC) have an ER/PR/HER2-negative molecular subtype and constitute the most difficult subtype to treat. Since treatment options vary

depending on the stage of breast cancer and which molecular subtype it is, uncovering genetic and molecular factors specific to the molecular subtype, such as RNA methylation, is very important to decide on the most appropriate treatment options (Lee 2023).

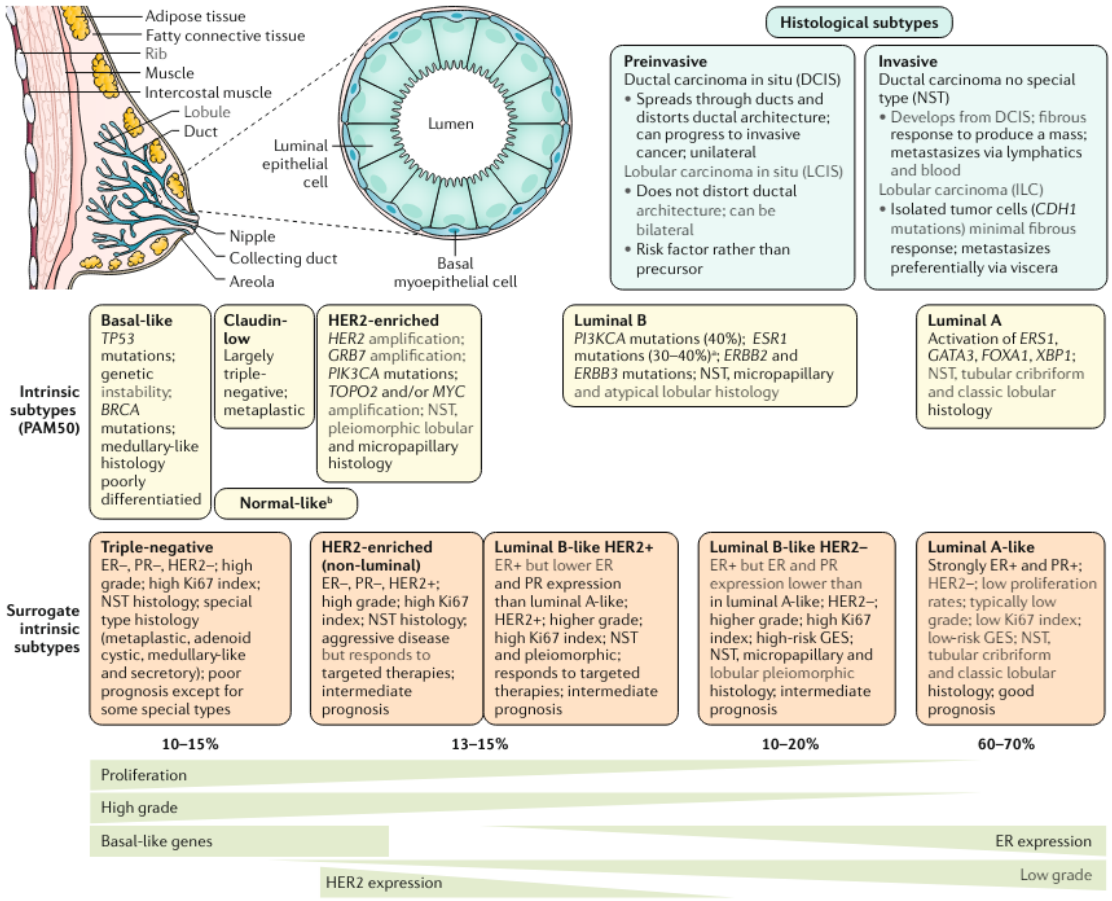


Figure 1.1. Breast Cancer Subtypes

(Harbeck et al. 2019)

Lifestyle and environmental factors play an important role in the development of breast cancer. As a matter of fact, 20% of breast cancer cases are attributed to preventable environmental factors such as smoking, exposure to sunlight, obesity and alcohol consumption (Danaei et al. 2005). Mechanistically, it has been reported that both the clonal evolution model, which can be explained as the gene mutations that induce cell differentiation and phenotypic regression with loss, uncontrolled proliferation and fail to activate cell death, and the cancer stem cell (CSC) model, which supports the immature cancer cells that can start cancer development, may play a role in the formation of breast cancer, and it has also been suggested that cancer stem cells can evolve clonally

(Bombonati and Sgroi 2011). In addition, several genes related with cancer development are operable with their known mutations including TP53, MYC, ERBB2, PTEN, and CCDN1 (Nik-Zainal et al. 2016). For this reason, mutations in genes such as PTEN, NGO1, TP53, and ATM, as well as BRCA1 and BRCA2, are used to assess the susceptibility to hereditary breast cancer (Taylor et al. 2019).

## 1.2. Epitranscriptomics

Epitranscriptomics, also called RNA epigenetics, is an exciting research field encompassing various RNA modifications and their functions, analogous to epigenetic modifications on DNA. Epitranscriptomics examines the effect of chemical changes on RNA without any difference in the RNA sequence. These modifications are able to diversify the secondary structure of RNAs and exist not only on messenger RNAs (RNAs) but also on ncRNAs, such as transfer RNAs (tRNAs), ribosomal RNAs (rRNAs), small nuclear RNAs (snRNAs), small nucleolar RNAs (snoRNAs), microRNAs (miRNAs), and long noncoding RNAs (lncRNAs) (Esteller and Pandolfi 2017; Roundtree et al. 2017). RNA was first discovered to have chemical modifications such as pseudouridine (Ψ), a structural isomer of uridine in late 1940s followed by the discovery of deoxy 5-methylcytosine in 1960s (Hotchkiss 1948; Cohn 1960). Currently, over 170 RNA modifications have been reported, including methylation, acetylation, uridylation and RNA editing of pseudouridine (Ψ) and adenosine-to-inosine (A-to-I). These dynamic modifications are involved in various molecular pathways such as RNA stability, secondary structure, translation, nuclear export and regulation of ncRNAs (Sağlam and Akgül 2024a). The methylation of RNAs was firstly identified on mRNAs in 1970s in various cell types (Desrosiers, Friderici, and Rottman 1974; Wei, Gershowitz, and Moss 1975).

Heretofore, approximately 13 of the 170 modifications discovered constitute methylations located on ribonucleotides. The most common types of methylation include $N^6$-methyladenosine ($m^6A$), $N^1$-methyladenosine ($m^1A$), 5-methylcytosine ($m^5C$), $N^6$,2′-O-dimethyladenosine ($m^6A_m$), $N^7$-methylguanosine ($m^7G$) (Figure 1.2) and are located in the various positions such as coding sequences (CDS), 5’untranslated region (5’UTR), 3’untranslated region (3’UTR), introns and adjacent to the cap (Motorin & Helm, 2011; Sağlam & Akgül, 2024). Methyl moieties may be deposited or reversible removed from

mRNAs in response to environmental or cellular cues, which governs the cellular fate. The molecular impact of RNA methylations includes, but not limited to, alternative splicing, mRNA translation, RNA stability, nuclear export of RNA and liquid–liquid phase separation (Zhenzhen Chen et al. 2022; Qiao et al. 2023; Ries et al. 2019). Consequently, such biochemical modifications affect various physiological changes such as stem cell fate determination or embryonic development can be affected and may lead to some disorders and diseases like cancer if deregulated (Alasar et al. 2022; Akçaöz-Alasar et al. 2024; Zhao et al. 2021).

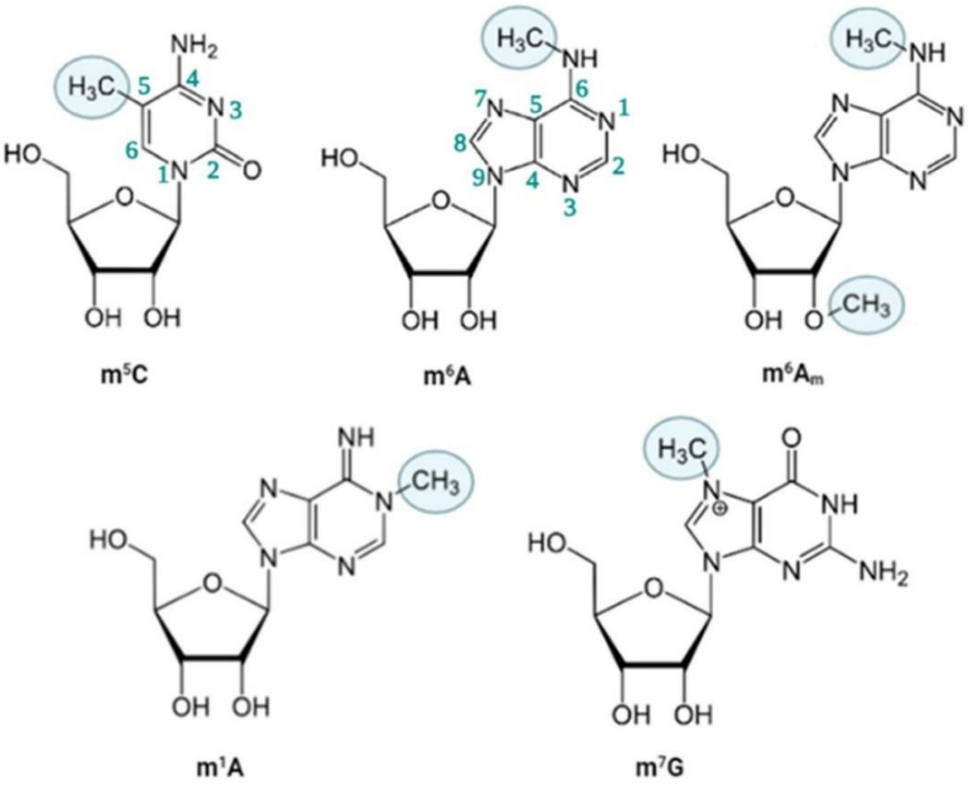


Figure 1.2. The types of RNA methylations
(Sağlam and Akgül 2024b)

## 1.3. The regulation and function of $N^6$-methyladenosine

RNA methylations are mainly named based on their position on the RNA molecule and the nucleotide that they are located in. $N^6$-methyladenosine, also called $m^6A$, is the methylated adenosine, which carries a methyl moiety on the nitrogen attached to the sixth carbon atom. The consensus sequence of $m^6A$ is a highly conserved

RR($m^6A$)CH motif in which R represents G or A, and H represents U, C or A (Dominissini et al. 2012). $m^6A$, the most common type of methylation discovered and studied since 1970s, was reported first in rRNA and tRNA of yeast cells (Starr and Sells 1969). $m^6A$ has also been reported in different organisms such as mammals, *Arabidopsis and Drosophila* (Jonkhout et al. 2017). $m^6A$ is a well-studied RNA modification mostly located in CDS, 3'UTR and 5'UTR (Roundtree et al. 2017). Since it is one of the most intense modifications within the cell and can be found in many RNA locations, it is a modification that plays various roles in many physiological and pathological processes including stress responses, circadian rhythms, stem cell differentiation, neurological and cancer diseases (Engel et al. 2018; H. Wu and Yi 2006).

$m^6A$ has a very dynamic and reversible mechanism with various regulatory proteins classified in three main protein clusters as writer, eraser and reader proteins. Firstly, writer proteins, methyltransferases, which function as a heterodimer, form a writer complex composed of Methyltransferase Like 3 (METTL3), Methyltransferase Like 14 (METTL14), Wilms Tumor 1-Associated Protein (WTAP), RNA Binding Motif Protein 15 (RBM15) and Zinc Finger CCCH-Type Containing 13 (ZC3H13). In the writer complex, METTL3 harbors the catalytic activity with an Adomet binding site and a catalytic domain to deposit the $m^6A$ moeity. METTL14 is a necessary writer protein for increasing the binding efficiency by stabilizing the METTL3 protein as a heterodimer. The other regulatory proteins of the complex include WTAP that facilitates the recruitment of other methyltransferases to the target mRNA and RBM15 that has a role in making interactions with other methyltransferases (Garcias Morales and Reyes 2021). Additionally, vir-like $m^6A$ methyltransferase associated protein (KIAA1429 or VIRMA) and RBM15B are known as the accessory proteins that dictate the target transcripts. The exact mechanism for the writer complex of $m^6A$ has not been completely illuminated, yet relatively better understood compared to other methylation types (Qian et al., 2019; Zaccara et al., 2019).

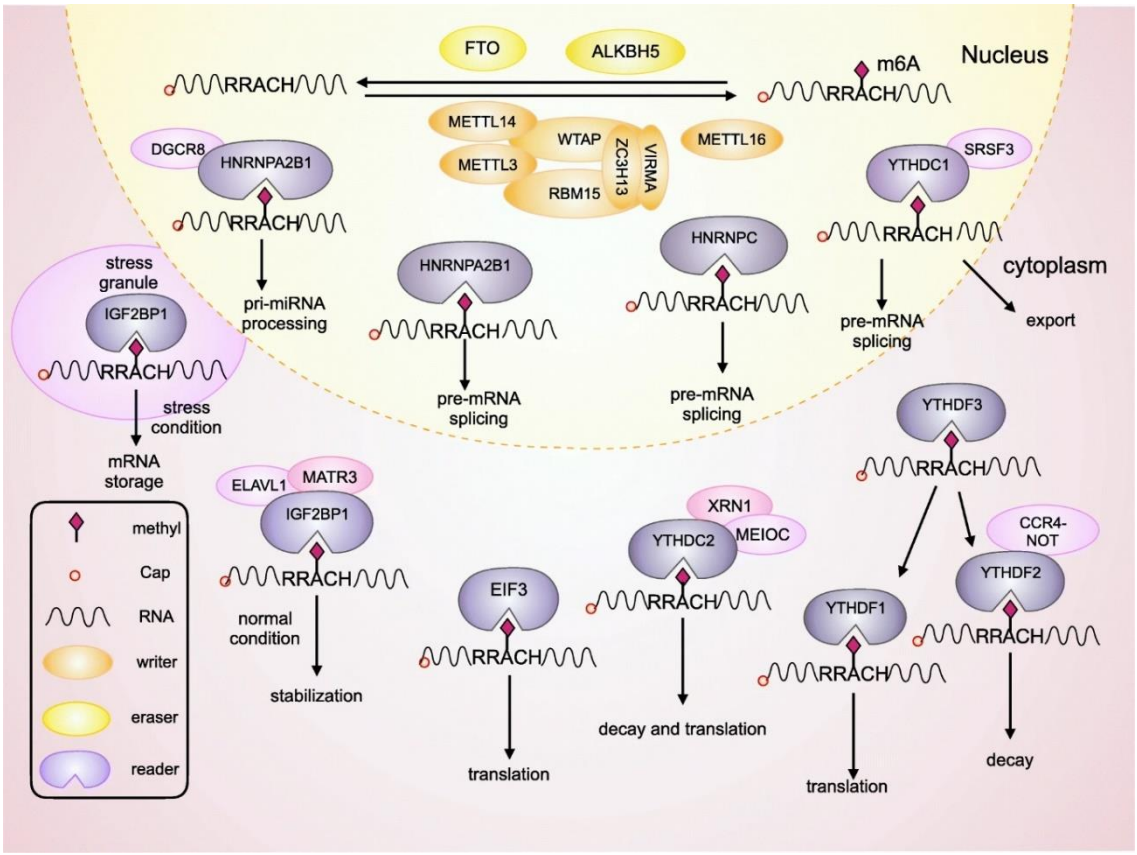


Figure 1.3. The dynamic mechanism of m$^6$A methylation and their downstream effects (He et al. 2019)

The eraser proteins, also known as demethylases, are responsible for the removal of the m$^6$A marks. So far, two most-studied eraser proteins have been reported, namely, alpha-ketoglutarate-dependent dioxygenase homolog 5 (ALKBH5) and fat mass and obesity-associated protein (FTO). Both can be classified as Fe(II)/α-ketoglutarate-dependent dioxygenases and catalyze the removal of m$^6$A modifications by oxidative demethylation (Jia et al. 2008; Zheng et al. 2013).

Readers are proteins that determine the fate of cells (Figure 1.3) and divided into two classes based on their mode of recognition: (1) direct readers that recognize m$^6$A modification by binding and (2) indirect readers that recognize the availability of m$^6$A due to the change in the secondary structure to recruit other reader proteins. Direct readers include YTH domain-containing proteins (YTHDC), YTH domain-containing family proteins (YTHDF), eukaryotic initiation factor 3 (elF3). Examples of indirect readers are heterogeneous nuclear ribonucleoprotein C (HNRNPC), heterogenous nuclear ribonucleoprotein G (HNRNPG), Insulin-like growth factor mRNA-binding protein (IGF2BP) and Fragile X Mental Retardation Protein (FMRP). YTHDC1, which regulates

splicing and the nucleocytoplasmic transport of mRNAs, and YTHDC2, which modulates translation and degradation of mRNAs, preferentially bind to the $m^6A$ portion of RNA(Patil et al. 2016; Wojtas et al. 2017). YTHDF1, YTHDF2 and YTHDF3 proteins located in the cytoplasm preferentially bind to $m^6A$ moieties and trigger various diseases if disregulated (Shi et al. 2017; Zong et al. 2021; J. yan Wang and Lu 2021). While the indirect reader proteins HNRNPC and HNRNPG bind to target RNAs and affect splicing. IGF2BP1, IGF2BP2 and IGF2BP3 proteins bind weakly to the $m^6A$ moiety and render stability to the methyl-adenine interaction. FMRP protein recognizes N6-methyladenosine on mRNAs and indirectly supports stability by recruiting YTHDF2 onto $m^6A$-methylated transcripts. As mentioned above, writer, reader and eraser proteins affect processes such as mRNA stability, localization and splicing within the cell, and their connection with cancer can be examined based on these and by observing gene expression levels (Berlivet et al. 2019).

## 1.4. The regulation and function of $N^1$-methyladenosine

$N^1$-methyladenosine ($m^1A$) is a type of RNA modification that has a methyl group attached to the nitrogen atom at the first carbon of adenine base. This modification occurs mostly in tRNA and rRNA as reported in 2012 and 2013, respectively (El Yacoubi, Bailly, and De Crécy-Lagard 2012; Sharma et al. 2013). The first mention of $m^1A$ methylation on mRNA came about in 2016. The researchers demonstrated the first comprehensive mapping and detection of $m^1A$ methylation in mRNA across various species. Furthermore, they also provided first evidence for its potential functional significance in mRNA regulation and cellular processes such as enhanced translation (Dominissini et al. 2016). As a consensus sequence, GUUCRA tRNA-like motif with T-loop-like structure was reported for $m^1A$ addition (X. Li et al. 2017). Then, the importance of $m^1A$ was demonstrated under several physiological situations through its roles in the RNA stability, translation efficiency, and other cellular processes (Zhang and Jia 2018).

As with every type of methylation, $m^1A$ also has a dynamic mechanism that involves writer, eraser and reader proteins. The heterodimeric TRMT61A/TRMT6 complex is the first writer protein reported to catalyze the $m^1A$ methylation of mRNAs. TRMT61A functions as the catalytic subunit, while TRMT6 serves as the regulatory unit. On the other hand, the mitochondrial RNAs also have TRMT61B and TRMT61C that are

responsible for the addition of $m^1A$ to the mitochondrial RNAs. The removal of $m^1A$ methylation is performed by the eraser proteins called as alpha-ketoglutarate-dependent dioxygenase homolog 1 (ALKBH1), alpha-ketoglutarate-dependent dioxygenase homolog 3 (ALKBH3), ALKBH5 and FTO demethylases (Zhuojia Chen et al. 2019; Liu et al. 2024a). YTHDF1, YTHDF2, YTHDF3 proteins can bind directly to $m^1A$ methylation and, especially, YTHDF3 has a functional role in the cell invasion and migration after $m^1A$ recognition. YTHDC1 and IGF1R proteins, which play a role in cell fate, serve as reader proteins. Current studies suggest that there might be other proteins that contribute to $m^1A$ methylation on mRNA and tRNA (Liu et al. 2024a; Jin et al. 2023).

## 1.5. $m^1A$ and $m^6A$ RNA methylation in breast cancer

Epigenetic changes contribute to the formation or progression of breast cancer. Changes in DNA methylation, genetic instability, and histone modifications are some of these epigenetic mechanisms and can be targeted for treatment (Sadida et al. 2024; Bennett and Licht 2018). Studies conducted in recent years show that not only protein-coding genes but also epitranscriptomic changes such as $m^1A$ and $m^6A$ methylation that occur on mRNAs play a very significant role in breast cancer pathology (Kumari, Groza, and Aguilo 2021). The writer, eraser and readers proteins can have oncogenic roles in proliferation and metastasis (Esteva-Socias and Aguilo 2024; Duan et al. 2024). Due to its much higher frequency in eukaryotic cells, current research has primarily focused on $m^6A$ methylation, and there is very limited information about $m^1A$ methylation. For instance, in the case of $m^6A$, the removal of $m^6A$ methylation on the apoptotic BNIP3 transcript by the m6A deletion protein FTO in MDA-MB-231 breast cancer cells leads to degradation of the BNIP3 transcript and therefore tumor growth and process metastasis (Niu et al. 2019). It has also been reported that $m^6A$ methylation of the BCL-2 transcript in MDA-MB-231 and MCF breast cancer cells, which have high expression of METTL3 compared to healthy cells, leads to increased translation efficiency of the relevant transcript and therefore tumor formation because of inhibition of apoptosis (H. Wang, Xu, and Shi 2020). Breast cancer metastasis to brain was also shown to be promoted by the YTHDF3 reader protein inducing of $m^6A$-enriched gene transcripts (Chang et al. 2020). In another study that involved interactions among METTL14, ALKBH5 and KIAA1429 and breast cancer formation only at the gene expression level, it was

suggested that METTL3 and METTL14 may contribute to breast adenocarcinoma pathology as demonstrated through studies conducted in MDA-MB-231 breast cancer cell line (L. Wu et al. 2019).

In the case of $m^1A$ methylation, removal of $m^1A$ from CSF-1 (Macrophage Colony Stimulating Factor 1) mRNA increases of CSF-1 mRNA stability with the help of ALKBH3 overexpression, which results in the cell invasiveness of BT20 breast cancer cells (Woo and Chambers 2019). It has also been reported that overexpression of TRMT6 increases cell proliferation and migration of breast cancer cells. When all this information is evaluated, it shows that $m^1A$ and $m^6A$ methylations play a critical role in the pathogenesis of breast cancer (Liu et al. 2024b; Fang et al. 2022). However, HCC1143 - triple negative breast cancer (TNBC) cell is almost a naive area for research including the effects of epitranscriptomic regulations on TNBC. The effects of $m^1A$ and $m^6A$ methylations have not been reported in HCC1143 cell lines.

## 1.6. Aim

This study aims to determine and compare the phenotypic effects of $m^6A$ and $m^1A$ methylated RNA transcriptome of HCC1143 cells after the knock-down of writer proteins METTL3 and TRMT61A.

# CHAPTER 2

# MATERIALS and METHODS

## 2.1. Cell culture and transfection

HCC1143 cells were kindly gifted from Erson-Bensan Laboratory in METU, Turkey, and cultured in DMEM-F12 (with 2 mM L-Glutamine, Gibco) media containing 10% fetal bovine serum (FBS) (Gibco) at 37°C and 5% $CO_2$. Additionally, the treated cells were collected by harvesting with Trypsin-EDTA (Gibco, 0.25%) and the washing steps were performed by 1x Phosphate-buffered saline (PBS) (Gibco).

The transfection of cells was performed by using si-METTL3 (Dharmacon) and si-TRMT61A (Dharmacon). In this procedure, off-target si-RNA (Dharmacon) was used as negative control of the ensuing experiments. To obtain a final concentration as 25 nM of siRNA, 100 µM stock siRNA solutions were stored at -20 °C after preparing with the 1X siRNA buffer (Dharmacon) [60 mM KCl (Sigma), 6 mM HEPES-pH 7.5 (Gibco), and 0.2 mM $MgCl_2$ (Applichem)].

$4 \times 10^5$ cells/dish HCC1143 cells were plated on the 10-cm dishes (Sarstedt) and incubated overnight at 37°C in 5% $CO_2$. 4 µl of DharmaFECT transfection reagent (Dharmacon) was used combined with 796 µl serum-free DMEM-F12 (Gibco) medium and 2 µl of 100 µM siRNA was added to 798 µl serum-free DMEM-F12 medium. After 5 min incubation at room temperature, diluted DharmaFECT transfection reagent solution was added into the siRNA solution. This mixture was also incubated at room temperature for 20 min after pipetting several times. Then, 6400 µl of DMEM-F12 medium with 10% FBS was replaced with old media in the dish and 1600 µl of final mixture was added clockwise as droplets onto the cells. Lastly, the cells were incubated at 37°C in 5% $CO_2$ for 72 hours. All experiments were performed as three replicates and p values were determined by student's t-test.

## 2.2. RNA-Seq analysis

Total RNAs were isolated from transfected HCC1143 cells by RNeasy Midi Kit (QIAGEN) according to manufacturer's protocol. RNA purities were examined with

agarose gel electrophoresis followed by RNA Sequencing performed by RefGen Biotechnology. The DEGs were further analyzed by Gene Ontology (GO) Enrichment Analysis such as biological process, molecular function and further cellular components tools. The most significant pathways were determined using genes differentially expressed 1.5-fold smaller or greater.

## 2.3. Colorimetric cell viability kit: WST8 assay

Cell viability was determined by using WST8 (a tetrazolium salt) (NutriCulture), which is a slightly yellow solution and reduced by cellular dehydrogenases to an orange formazan product. Therefore, WST8 reduction is directly related to the viability of the cells. The viability assay by WST8 was performed by addition of 10 µl of WST8 solution into the 96-well plate with transfected cells for 48h, 72h and 96h. After 2-hour incubation in living conditions of HCC1143 at 37°C and 5% $CO_2$, absorbance at 450 nm was measured by UV Spectrometer (Multiskan FC, Thermo Scientific).

The absorbance of the blank group, the samples containing media with 10% FBS, was subtracted from the measurements and cell viability was determined by the following formula (Kamiloglu et al. 2020). The control group included nontreated cells. For the calculation of viability, the following formula was applied: Cell viability (%) = (absorbance value of sample/absorbance value of control) × 100.

## 2.4. Cell cycle analysis

After trypsinization of cells and centrifugation at 1200 rpm for 5 min at 25˚C, the supernatant was discarded and the cell pellet was dissolved in 1 ml of cold PBS. Then, 4 ml of cold absolute EtOH (Merck) was slowly and continuously added while vortexing to fix the cells. After the fixation, cells were stored at -20˚C for at least 3 days (Pozarowski and Darzynkiewicz 2004).

For propidium iodide (PI) staining, the fixed cells were centrifuged at 1200 rpm for 10 min at 4˚C and the pellet was dissolved in 5 ml of ice-cold PBS. After centrifugation in the same conditions, the pellets were completely purged from the EtOH. Then, 200 µl of 0.1% Triton-X-100 in PBS was used to dissolve pellets and 20 µl of 200 µg/ml RNase A was added. After incubation at 37˚C for 30 min, 20 µl of 200 µg/ml of

PI was added and incubated for 15 min at 25˚C in the dark. Samples were then analyzed by flow cytometry (FACSCanto$^{TM}$, BD). The population density in each cell cycle phase was calculated by ModFit LT$^{TM}$ software.

## 2.5. Apoptosis measurement

The rate of apoptosis was analyzed by flow cytometry (FACSCANTO, BD) by using Annexin V-FITC and 7AAD-PerCP (BD) dyes. Media containing the suspended cells were also collected while trypsinization, and samples were centrifuged at 1500 rpm for 5 min at room temperature. The resulting pellet was washed with 1X PBS, and supernatant was discarded after centrifugation. Pellet was dissolved with 50 µl of annexin binding buffer (1X) (BD) and stained with 10 µl of Annexin V-FITC and 10 µl of 7AAD-PerCP to differentiate the early apoptotic, late apoptotic and death cells in flow cytometry. The cells were incubated at room temperature for 15 min in the dark and diluted by using 200 µl 1x PBS (Gibco). Unstained and monochrome-stained samples were used as compensation controls. Based on staining characteristics, Annexin V + / 7AAD – cells were considered as early apoptotic while Annexin - / 7AAD + cells were represented the dead cells. Additionally, the cells, which were stained with both dyes, were marked as the late apoptotic cells. However, if the cells were not stained with any of these dyes, they were labeled as live cells.

## 2.6. Total RNA isolation

Cell pellets were dissolved in GeneAll® RiboEx™ according to the manufacturer's protocol (5~10 x $10^6$ cells in 1 ml RiboEx$^{TM}$). After the incubation at room temperature for 5 min, 0.2 ml (1:5) of chloroform (Sigma) was added and shaken vigorously. After 2 min incubation at room temperature, the homogenate was centrifuged at 12,000 × g for 15 min at 4ºC. The aqueous phase on the top of the tube was cautiously transferred into a new tube to separate the phase with RNA. Then, 0.5 ml (1:2) of absolute isopropanol (Sigma) was added and incubated for 10 min at room temperature to precipitate RNAs with centrifugation at 12.000× g for 10 min at 4°C. For washing step, 1 ml of (1:1) 75% ice-cold ethanol (Merck) was added after ensuring that all isopropanol is removed from the environment. Following centrifugation at 7500 × g for 5 min at 4°C

and removal of EtOH from the pellets, the RNA pellets were air-dried entirely for 5-10 min. Lastly, the RNA pellets were dissolved with 20 µl of nuclease-free water (Gibco) and stored at -80°C until use.

NanoDrop Spectrophotometer (Thermo Fisher Scientific) was used to measure RNA concentrations. The samples with the absorbance ratios of 260/280 and 260/230 equal to or greater than 2, were utilized for further experiments. RNAs were also fractionated on 1% agarose gel to assess their integrity. The agarose gel electrophoresis was performed in TBE buffer (Tris-borate-EDTA buffer, 890mM Tris-borate, 890mM boric acid, 20mM EDTA). The gel images were captured by using ChemiDoc MP (Bio-Rad) with the aid of UV light.

## 2.7. Colorimetric $m^6A$ detection

To determine the total m6A level on RNA, EpiQuik™ m6A RNA Methylation Quantification Kit (Colorimetric) was used according to the manufacturer's protocol. Optimal samples consisted of 200 ng RNA per replicate, and two replicates were used. Standard curve was previously prepared with positive controls and negative controls and used to calculate the percentage of $m^6A$ on total RNA. Firstly, 2 µl of total RNA (200 ng ) was added onto the strip wells for each sample followed by addition of 80 µl of Binding Solution (BS). Then, the samples were incubated at 37°C for 90 min. After removing BS, 150 µl of Wash Buffer (WB) was added and removed for three times. 50 µl of 1:1000 diluted capture antibody was added and washed with WB for three times after incubation at room temperature for 60 min. Then, 1:2000 diluted 50 µl of Detection Antibody was added and incubated at room temperature for 30 min, followed by washing with 150 µl of WB. Samples were incubated at room temperature for 30 min after addition of 1:5000 diluted 50 µl of Enhancer Solution and washed with WB for five times. Lastly, 100 µl of Developer Solution and Stop Solution were added, respectively when the bright blue color was observed in the samples. The absorbance of the samples was determined at 450 nm by Microplate reader (Multiskan FC, Thermo Scientific). For $m^6A$ percentage calculations, [Sample OD (optical density) – NC OD] was divided by the slope of standard curve to determine the $m^6A$ amount in ng and $m^6A$ amount was divided by the amount of input sample RNA in ng.

## 2.8. FTIR (Fourier Transform Infrared Spectroscopy)

FT-IR (Perkin Elmer, UATR Two) spectroscopy used to analyze total RNA including an attenuated total reflection (ATR) unit and a MIR TGS (Mid-infrared Triglycine Sulfate). The FT-IR spectra were performed by 32 co-added scans at a 2 $cm^{-1}$ spectral resolution in the wavenumber range of 4000-800 $cm^{-1}$ at room temperature. As a background, air spectrum was recorded after cleaning of ATR. Approximately 2000 ng of 2 µl total RNA was measured on the ATR diamond crystal and dried in dry air purge at room temperature for about 8 min as three replicates. The OH stretching mode (4000-3000 $cm^{-1}$) was used to control of appropriate removal of water. For data analysis, the 'OPUS 7.0' (Bruker, Germany) and 'Kinetics' software running under MATLAB were used, as described previously (Güler et al., 2016b, 2011; Vorob'ev et al., 2023). Then, absorbance spectrums were baseline-corrected by interpolating lines between spectrum points at multiple wavenumbers as 3970, 3715, 2800, 2500, 1800, 1750, 1510, 1438, 1315, 946, 895, 835, and 801 $cm^{-1}$. Calculation of second derivative spectrum was carried out by using the average absorbance spectrum in the Savitzky-Golay algorithm with 9 smoothing points to sort out the superimposed bands. FTIR analyses were performed by Onur Akkuş and Asst. Prof. Dr. Günnur Güler from the Physics Department of Izmir Institute of Technology.

## 2.9. cDNA synthesis and quantitative PCR (qPCR)

Thermo Scientific RevertAid First Strand cDNA Synthesis Kit (Thermo Fisher Scientific) was used to synthesize cDNA according to manufacturer's protocol. 4 µl of 5X Reaction Buffer, 1 µl Random Hexamer primer, 2 µl of 10 mM dNTP mix, 1 µl of RiboLock RNase Inhibitor and 1 µl of RevertAid M-MuLV Reverse Transcriptase were added sequentially in a tube containing 1000 ng of RNA. Following a quick spin, the reaction was carried out by using thermal cycler (Blue-Ray) with the following conditions: 5 min at 25°C, 60 min at 42°C and 5 min at 70°C. For dilution of total 20 µl of cDNA into 5 ng/µl, 180 µl of nuclease-free water was added and kept at -80°C.

For the quantitative PCR, master mix was prepared with 6.25 µl of RealQ Plus 2x Master Mix (Ampliqon), 4.25 µl of nuclease-free water and 1 µl of 5 ng/µl cDNA per sample. Then, 1 µl of 5 µM forward and reverse primer stock was added to each reaction

tubes after distributing 11.5 µl of master mix to the reaction tubes. The incubation condition was applied as following: 2 min at 95°C for initial denaturation and 15 seconds denaturation at 95°C with 1 min annealing at 60°C for 45 cycles. GAPDH housekeeping gene was used for normalization. Experiment set-up was composed of two technical and three biological replicates for each sample. The primers used were listed in the Table 2.1.

Table 2.1. The list of primer sequences used in this study

| Genes | Forward 5'-3' | Reverse 5'-3' |
|---|---|---|
| **METTL3** | AGATGGGGTAGAAAGCCTCCT | TGGTCAGCATAGGTTACAAGAGT |
| **METTL14** | GAGTGTGTTTACGAAAATGGGGT | CCGTCTGTGCTACGCTTCA |
| **WTAP** | TTGTAATGCGACTAGCAACCAA | GCTGGGTCTACCATTGTTGATCT |
| **RBM15** | AAGATGGCGGCGTGCGGTTCCGCTGTG | AAGTTCACAAAGGCTACCCGCTCATCC |
| **FTO** | CTTCACCAAGGAGACTGCTATTTC | CAAGGTTCCTGTTGAGCACTCTG |
| **ALKBH5** | TCCAGTTCAAGCCTATTCG | CATCTAATCTTGTCTTCCTGAG |
| **YTHDF2** | CCTTAGGTGGAGCCATGATTG | TCTGTGCTACCCAACTTCAGT |
| **YTHDF3** | TGACAACAAACCGGTTACCA | TGTTTCTATTTCTCTCCCTACGC |
| **YTHDC2** | GTGTCTGGACCCCATCCTTA | CCCATCACTTCGTGCTTTTT |
| **IGF2BP2** | ATCGTCAGAATTATCGGGCA | GCGTTTGGTCTCATTCTGTC |
| **IGF2BP3** | AGACACCTGATGAGAATGACC | GTTTCCTGAGCCTTTACTTCC |
| **GAPDH** | ACT CCT CCA CCT TTG ACG C | GCTGTAGCCAAATTCGTTGTC |

## 2.10. Isolation of proteins and western blotting

Proteins were isolated by using 48 µl of 1X RIPA [radio immunoprecipitation assay solution: 25 mM Tris•HCl pH 7.6, 150 mM NaCl, 1% NP-40, 1% sodium deoxycholate, 0.1% SDS (CST) with a ratio of 1:100] and 2 µl of the protease inhibitor cocktail (100X) (CST). Cells were vortexed for 1 min four times in these components and then incubated on ice for 10 min. After centrifugation for 5 min at 12,000 × g at 4°C, the supernatant was transferred into a fresh tube. The concentration of proteins was determined with Bradford assay. To this extent, 3 µl of isolated protein was transferred into a new tube and diluted as 1:5 by addition of 12 µl of nuclease-free water. Firstly, 200 µl of Bradford solution was added into the wells of 96-well plate and 5 µl of the protein

sample was added and homogeneously mixed. Then, the concentrations were measured at 495 nm by UV Spectrometer (Multiskan FC, Thermo Scientific) after incubation in the dark for 5 min. Protein concentrations were calculated using a previously prepared standard curve that contains absorbance and concentration. The isolated proteins were placed at -20°C until use.

Proteins were fractionated on SDS-polyacrylamide gel (SDS-PAGE) that included 10% separating and 5% stacking gels. Briefly, 10% separating gel was prepared by mixing 1650 µl of 40% acrylamide mix, 2050 µl of distilled water, 75 µl of 10% APS, 5 µl of TEMED and 1250 µl of 4X Seperating Buffer [18.17 g of Tris base (Final conc. 1.5M), 0.4 g of SDS (Final conc. 0.4%), 100 ml of $dH_2O$, pH 8.8]. 5% stacking gel was then prepared by mixing 640 µl of 40% acrylamide mix, 2780 µl of distilled water, 75 µl of 10% APS, 5 µl of TEMED and 1250 µl of 4X Stacking Buffer [6.06 g of Tris base (Final conc. 0.5M), 0.4 g of SDS (Final conc. 0.4%), 100 ml of $dH_2O$, pH 6.8]. After polymerization of the separating gel, the stacking gel was poured onto separating buffer. 50 µl of protein extract was mixed with 5 µl of Laemmli buffer (Bio-Rad) with β-mercaptoethanol and heated for 5 min at 95˚C prior to loading into the wells. Protein ladder (New England Biolabs) was utilized to mark the size of the related proteins. β-actin was used as a loading control.

The running process was performed at 80 V until the proteins passed the stacking gel and then increased to 90 V for 2 hours in the METTL3 experiments and 3 hours in the TRMT61A experiments. Proteins were transferred onto PVDF membranes (Thermo Scientific) at 325 mA for 1 hour and 45 min. The blocking process was done by using 5% non-fat dry milk (CST) in 1X TBS-T (Tris Buffered Saline-1% Tween 20 (FISHER) buffer for 1 hour at room temperature. All washing processes after blocking, primary antibody and secondary antibody were performed 3 times for 5 min with 1X TBS-T buffer. The incubation with primary antibody was also performed overnight at 4°C as 1:1000, 1:2000 and 1:5000 for METTL3(CST), TRMT61A (ThermoFisher) and β-actin (CST), respectively. Lastly, the secondary antibody incubation was carried out for 1 hour at room temperature with anti-rabbit or anti-mouse IgG-HRP conjugate secondary antibody (CST) according to the manufacturer's recommendations. Pierce™ ECL Western Blotting Substrate (Thermo Fisher Scientific) was used as a chemiluminescent substrate to measure protein abundance on the membrane with the help of of ChemiDoc MP (Bio-Rad).

# CHAPTER 3

# RESULTS

## 3.1. Dynamic expression of writer, eraser and reader proteins in breast healthy and cancer cell lines

DSMZCellDive (Diving into high-throughput cell line data) was used to examine the expression patterns of genes in breast cells involved in $m^6A$ and $m^1A$ RNA methylation (Pommerenke et al. 2024). The expression patterns of writer, eraser and reader proteins were quite diverse based on cancer types compared to normal breast cells. For instance, FTO eraser protein is intensively higher in MDA-MB-468 cell line, an invasive ductal carcinoma that has ER, PR, and E-cadherin negative feature with mutated p53. IGF2BP1 reader protein is highly expressed in CAL-51 cell line, a progressive ductal breast adenocarcinoma which is a triple-negative breast cancer (Figure 3.1).

To examine the potential differences in the expression levels of the $m^6A$ related genes between healthy breast cells (MCF10A) and triple negative breast cancer cells (HCC1143), qPCR analyses were performed. RBM15 expression was 3.92-fold ($P < 0.0001$) and YTHDF3 ($P < 0.05$) was 1.5-fold higher in HCC1143 cells compared to MCF10A. METTL14 ($P < 0.001$), FTO ($P < 0.01$), IGF2BP2 ($P < 0.001$) and YTHDC2 ($P < 0.001$) were decreased approximately 2-fold in HCC1143 cell line compared to MCF10A (Figure 3.2).

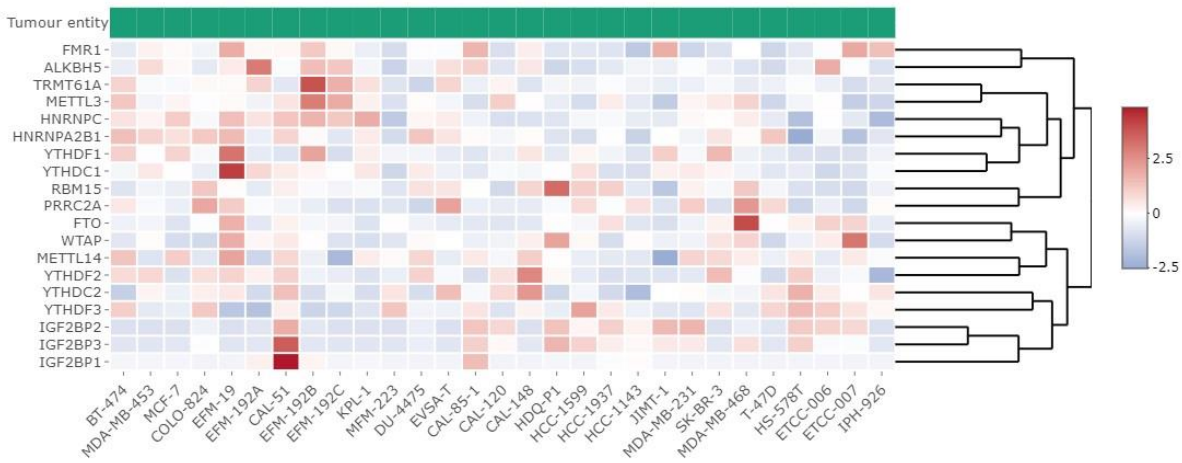


Figure 3.1. The heatmap of expression levels of $m^6A$ and $m^1A$ regulatory proteins

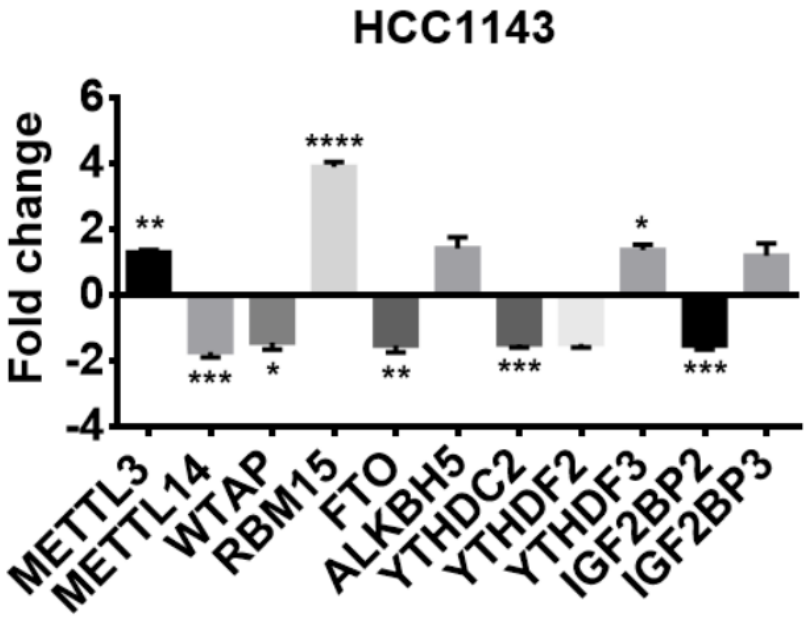


Figure 3.2. Expression analysis of various writer, eraser and reader proteins in HCC1143 breast cancer cell line. The data were normalized with MCF10A healthy breast cell line. Results represent mean ± SD of three independent experiments. Statistical analysis was carried out using student's t-test (**** $P < 0.0001$; *** $P < 0.001$; ** $P < 0.01$; *$P < 0.05$).

## 3.2. The expression level of METTL3 and TRMT61A in healthy and cancer breast cells

Western blotting was carried out to determine the protein expression level of $m^6A$ and $m^1A$ writers. Although there was no significant change in the METTL3 protein level between healthy and cancer breast cells, the TRMT61A protein level increased approximately 2-fold ($P < 0.001$) in HCC1143 cells compared to MCF10A healthy breast cells. Therefore, it was hypothesized that the knockdown approach can be used to examine the effects of $m^6A$ and $m^1A$ methylation in HCC1143 triple negative breast cancer cells. The aim was to compare the contribution of $m^6A$ and $m^1A$ RNA methylations in HCC1143 cell type characteristics (Figure 3.3).

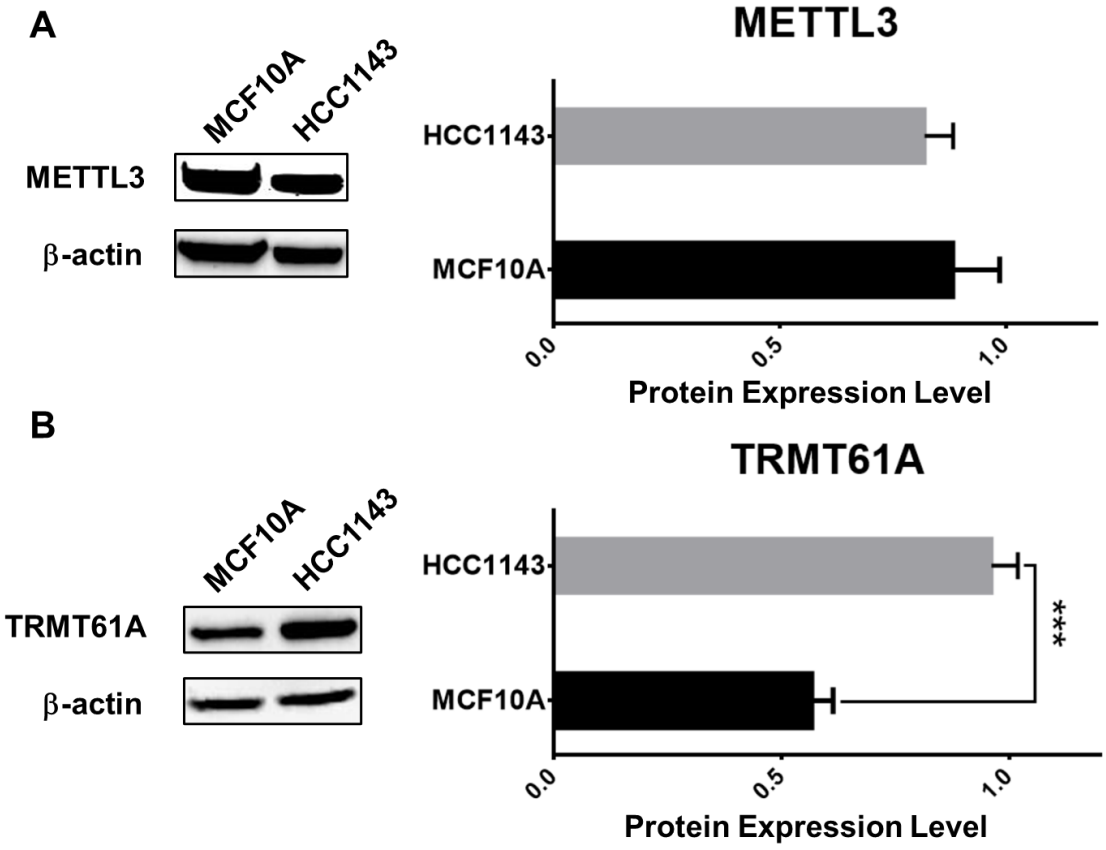


Figure 3.3. The protein level of (A) METTL3 and (B) TRMT61A in the MCF10A healthy breast cells and HCC1143 triple negative breast cancer cells. Mean ± SD of three replicates were used to represent on graphs. Student's t-test was used for statistical analyses (*** $P < 0.001$).

## 3.3. METTL3 and TRMT61A knock-down in HCC1143 cells

To silence the $m^6A$ writer protein METTL3 and $m^1A$ writer protein TRMT61A, HCC1143 triple negative breast cancer cells were transfected with 25 nM of si-METTL3, si-TRMT61A and off-target negative siRNA (si-NC). Off-target negative siRNAs were used as a negative control in both knock-down. After transfection with METTL3 and TRMT61A siRNAs, the silencing of METTL3 was achieved as 81.8% while it was 86.7% in the silencing of TRMT61A (Figure 3.4).

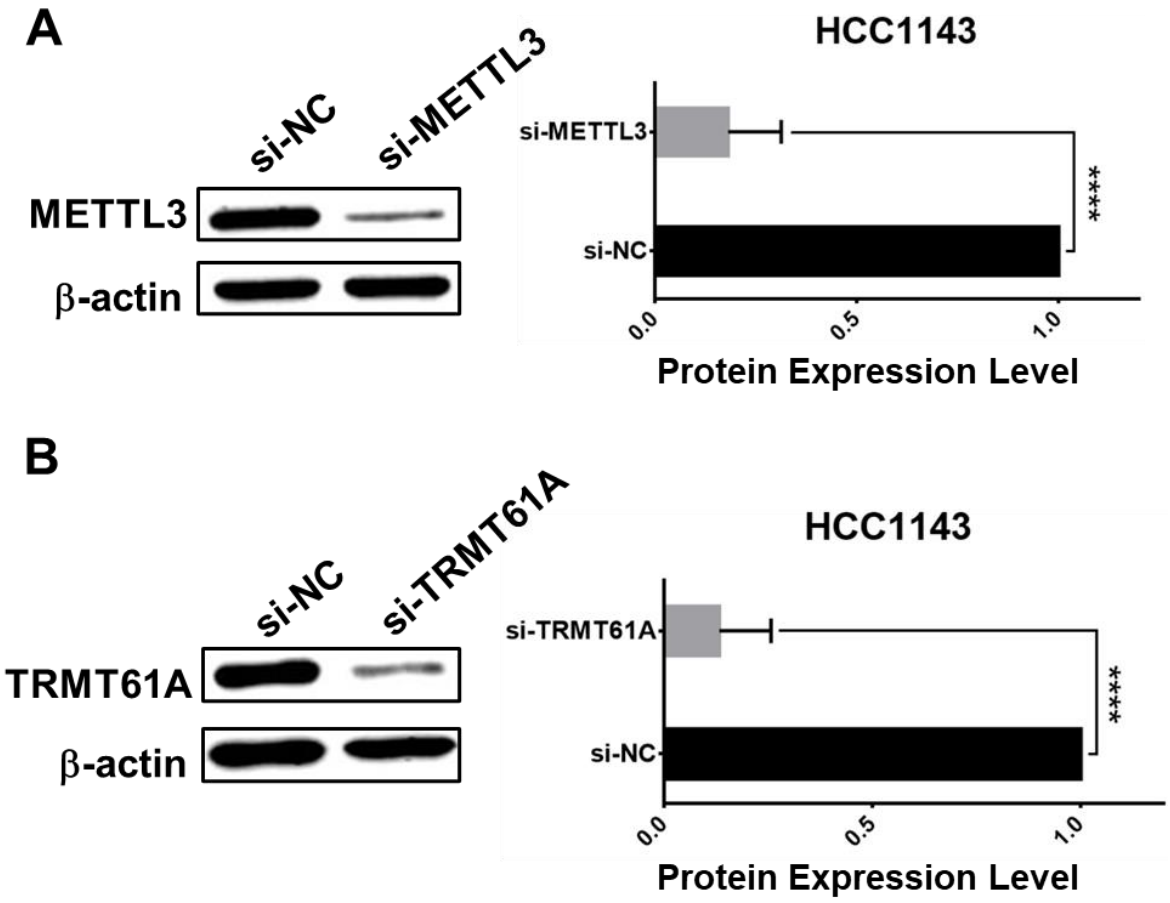


Figure 3.4. (A) The Western blot analysis after silencing of $m^6A$ writer protein, METTL3 (B) The Western blot analysis after silencing of $m^1A$ writer protein, TRMT61A. Histograms represent mean ± SD (n=3). Statistical analyses were carried out using student's t-test (**** $P < 0.0001$).

## 3.4. Total m$^6$A level detection after silencing of METTL3

To determine the maximum level of m$^6$A reduction after knock-down of METTL3. The m$^6$A level in total RNA in 48h, 72h and 96h post-transfection was analyzed by a colorimetric m$^6$A detection technique and the most reduction in the m$^6$A level of total RNA was observed as 41.2% after 72h transfection of HCC1143 cells. After 72h transfection, the METTL3 level was decreased by 81.8% (Figure 3.5).

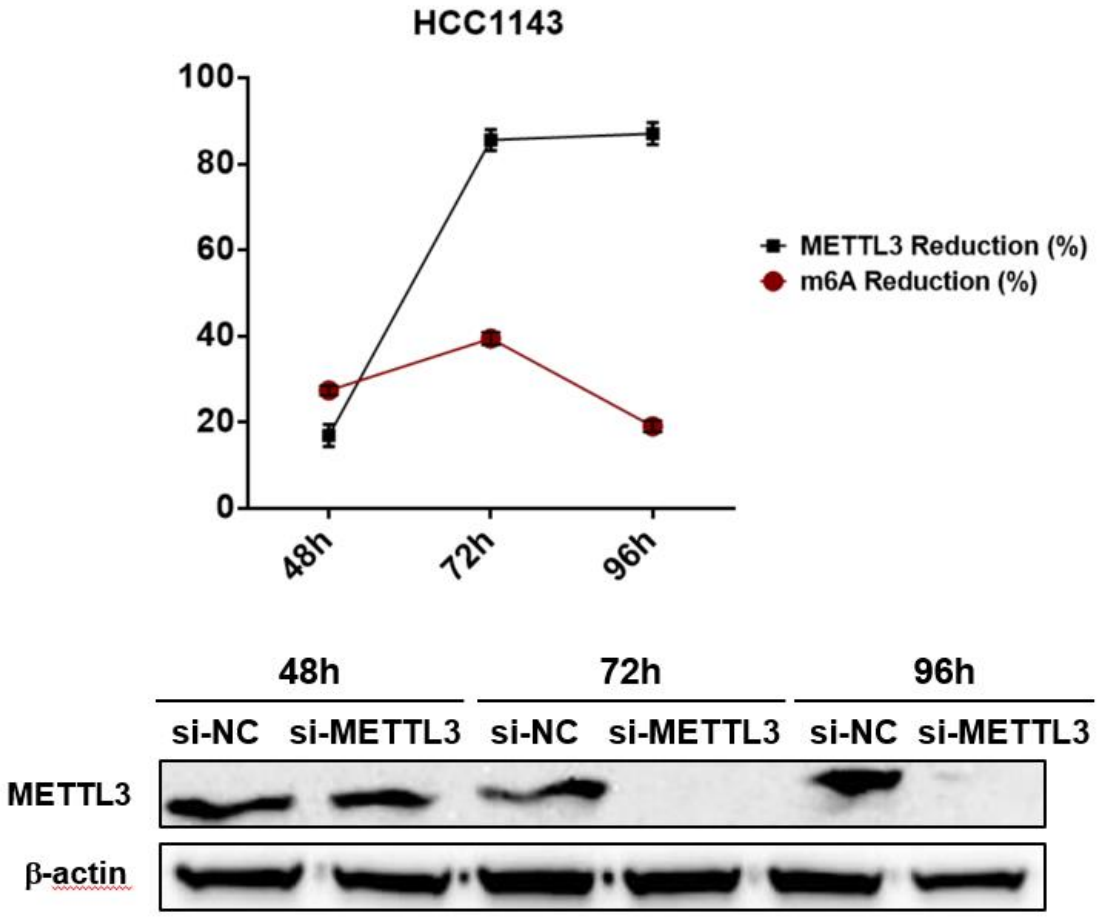


Figure 3.5. Total m$^6$A level detection results are shown in red circle that observed by a colorimetric m$^6$A detection technique and the protein expression level of METTL3 after 48h, 72h and 96h transfection that observed in western blot.

In addition to the colorimetric $m^6A$ kit, a novel technique for detection of total RNA methylation was performed by FTIR (Fourier-transform infrared spectroscopy) technique. The alteration of $CH_3$ and $CH_2$ peaks after METTL3 transfection was detected in HCC1143 cells by using FTIR spectroscopy. When asymmetric stretching of $CH_3$ and $CH_2$ at 2952 and 2925 $cm^{-1}$ were compared, the difference between the peak were higher in the METTL3 knocked-down HCC1143 cells. In a similar manner, the difference of $CH_3$ from $CH_2$ peaks was higher in symmetric stretching at 2869 and 2853 $cm^{-1}$ and asymmetric bending at 1489 and 1461 $cm^{-1}$ (Figure 3.6).

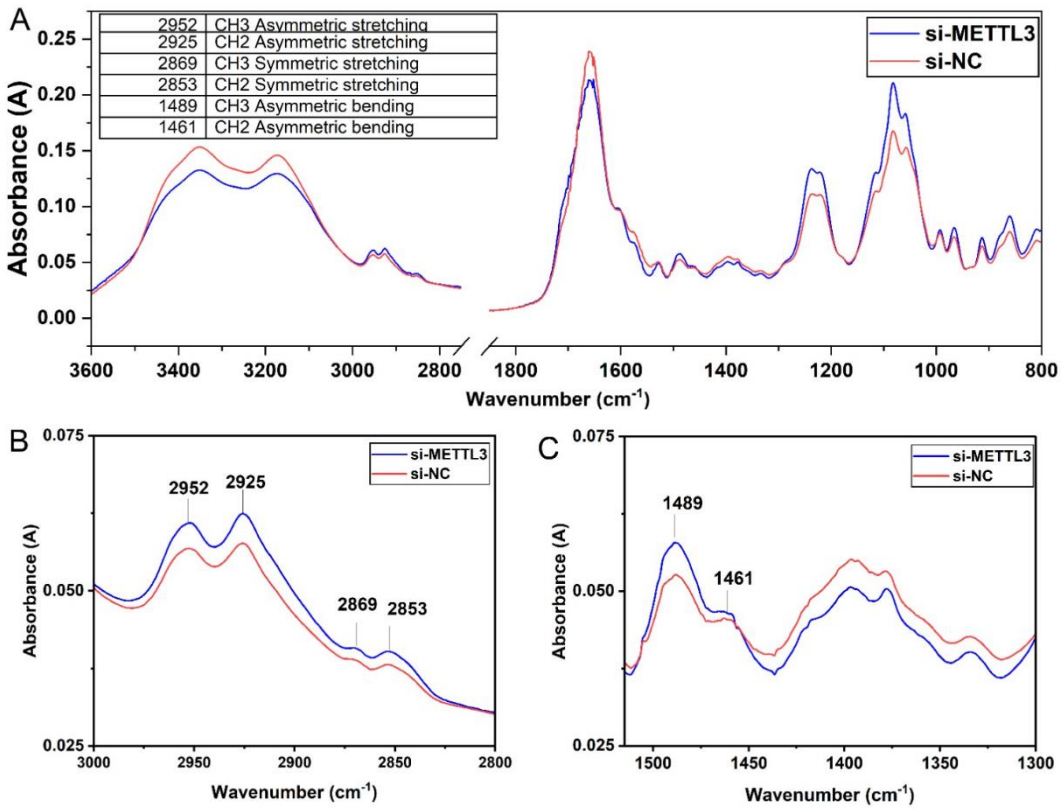


Figure 3.6. (A) FTIR analysis of METTL3 knocked-down HCC1143 cells and its negative control by focusing on between (B) 3000-2800 $cm^{-1}$ and (C) 1575-1300 $cm^{-1}$ wavenumbers.

## 3.5. Viability effect after decreasing of $m^6A$ and $m^1A$ methylations

To examine the phenotypic effects of the writer knockdown on HCC1143 cell viability, WST8 colorimetric viability detection procedure was carried out. In the case of $m^6A$ reduction, cell viability was assessed for 48h, 72h and 96h as 32.12%, 40.1% and 14.38% change, respectively. For all time points, viability of cells decreased significantly proportional to the $m^6A$ reduction. As observed previously, the most effective time for the decrease in cell viability was 72 hours. For this reason, TRMT61A silencing was carried out at the 72h time point resulting in decrease by 27.4% in the viability of the cells after the TRMT61A knock-down (Figure 3.7).

To check if the reduction in the viability of triple negative cells is associated with apoptotic cell death, flow cytometry analysis was performed. However, there was no significant change in the apoptotic rate of HCC1143 cells upon knockdown of either writer (Figure 3.8).

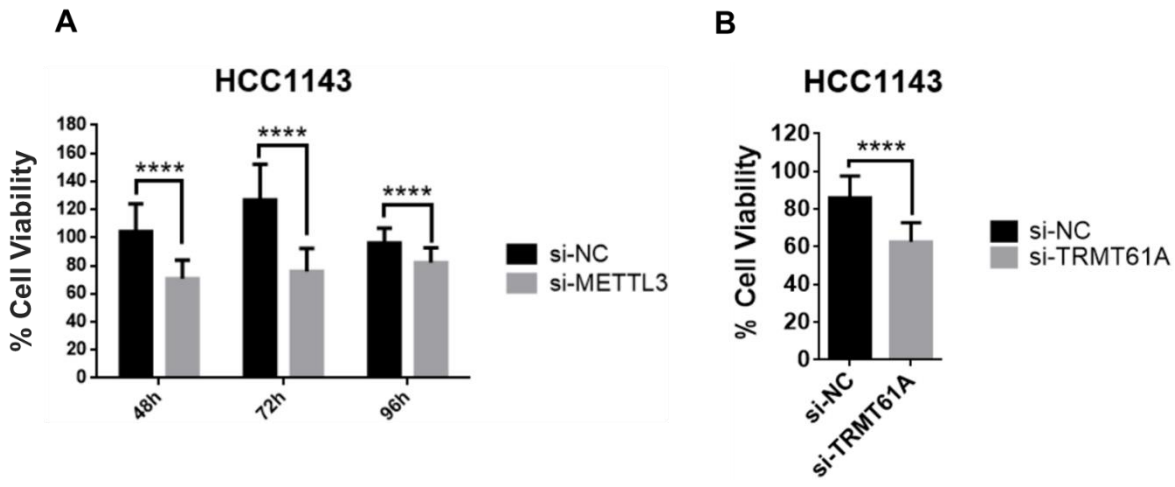


Figure 3.7. Viability assays of HCC1143 cells after (A) $m^6A$ reduction in 48h,72h and 96h and (B) $m^1A$ reduction for 72h. Histograms represent mean ± SD (n=3). Statistical analyses were carried out using student's t-test (**** $P < 0.0001$).

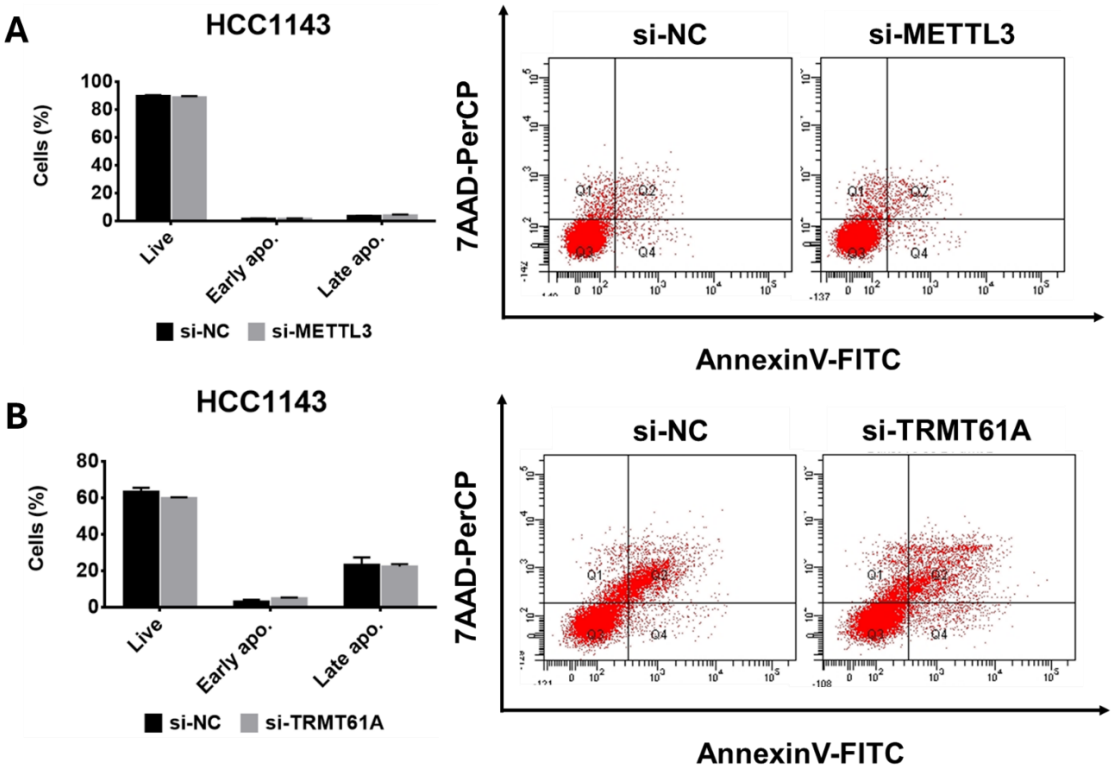


Figure 3.8. Flow cytometry analysis of (A) METTL3 and (B) TRMT61A transfected HCC1143 cells. Bars demonstrate the mean ± SD for three biological replicates. Statistical analyses were carried out using student's t-test.

## 3.6. The effect of silencing on the cell cycle mechanism

Knockdown of writer proteins leads to a reduction in cell viability. Therefore, it was hypothesized that the reduction in cell viability might be associated with an arrest in cell cycle check points. As expected, after the reduction of METTL3, there was a stall in G2/M phase. However, there was no significant difference in cell cycle phases upon the knockdown of TRMT61A in HCC1143 cells (Figure 3.9).

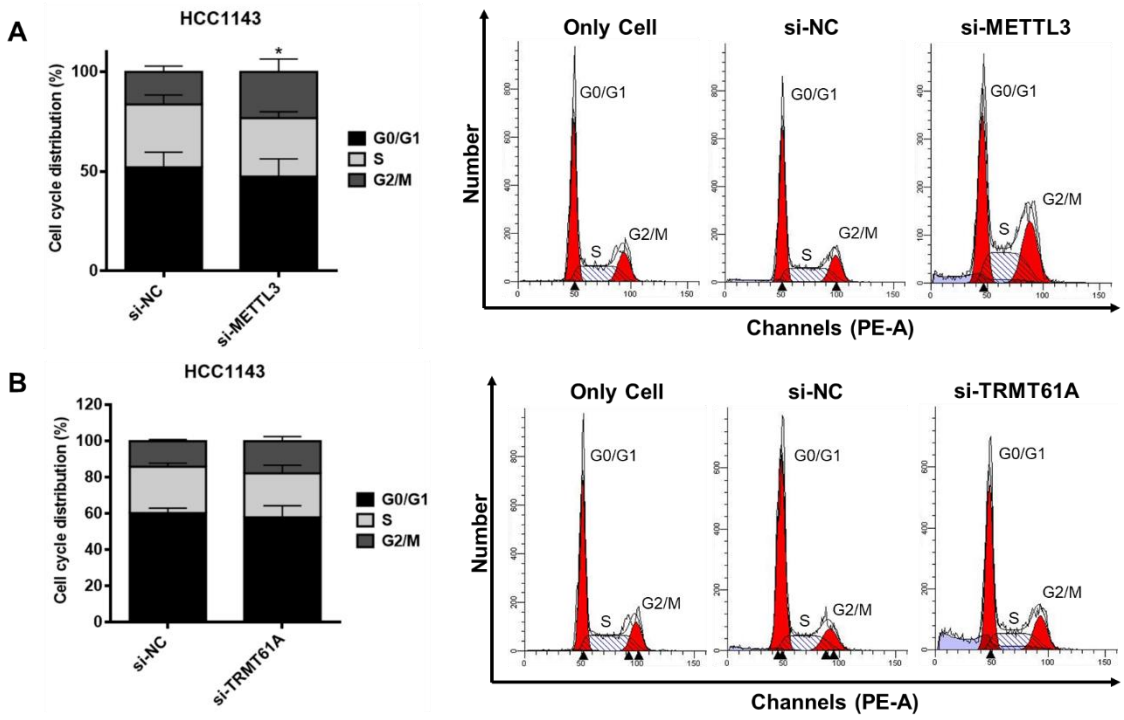


Figure 3.9. Cell cycle analysis of HCC1143 cells after knock-down of (A) METTL3 and (B) TRMT61A writer proteins. Data shows the mean ± SD for three biological replicates and student's t-test was used for statistical analysis (*P < 0.05).

## 3.7. RNA Sequencing and GO analysis of METTL3 and TRMT61A transfected HCC1143 cells

To uncover the effects of knockdown of $m^6A$ and $m^1A$ writers on gene expression patterns of HCC1143 cells, RNA sequencing was performed with total RNAs isolated from METTL3 and TRMT61A-silenced HCC1143 cells. To assess the purity of RNAs, 260/230 and 260/280 ratios were calculated, which appeared to be approximately 2. Additionally, the visual analysis of RNAs fractionated on 1% agarose indicated no detectable degradation (Figure 3.10-11).

In RNA-Seq results, the differentially expressed genes (DEGs), which have the fold changes greater or smaller than 1.5, were used to draw heatmap (Figure 3.12). Approximately 585 genes were detected in the METTL3-silenced HCC1143 cells. On the other hand, approximately 687 DEGs were detected in the TRMT61A-silenced HCC1143 cells. These genes were analyzed separately in Gene Ontology (GO) enrichment analysis

based on biological process (Figure 3.13), molecular function (Figure 3.14) and cellular component (Figure 3.15). Cell migration and enzyme-linked receptor protein signaling were the most significant biological process that determined in the GO analysis (Figure 3.13A). However, in si-TRMT61A samples, immune related and negative regulation of proliferation pathways were more prominent (Figure 3.13B).

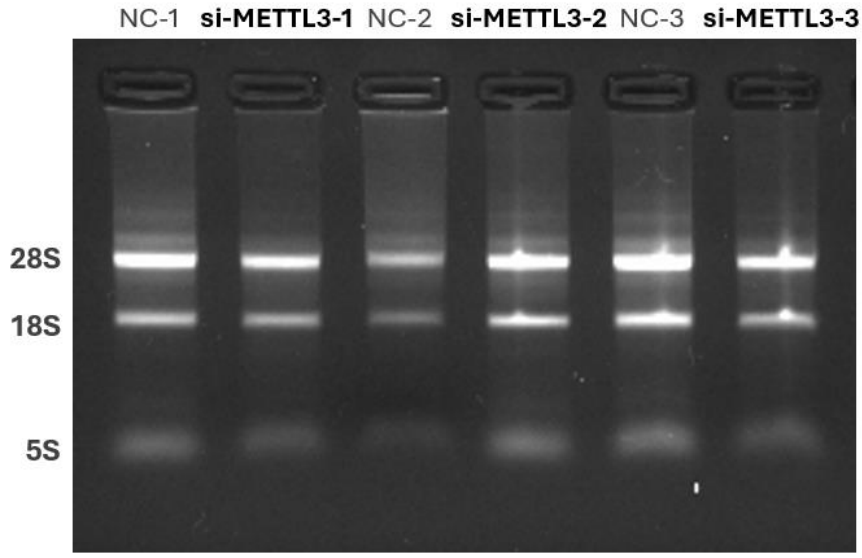


Figure 3.10. The agarose gel image of total RNAs isolated for RNA-Seq from NC and METTL3-transfected HCC1143 cells

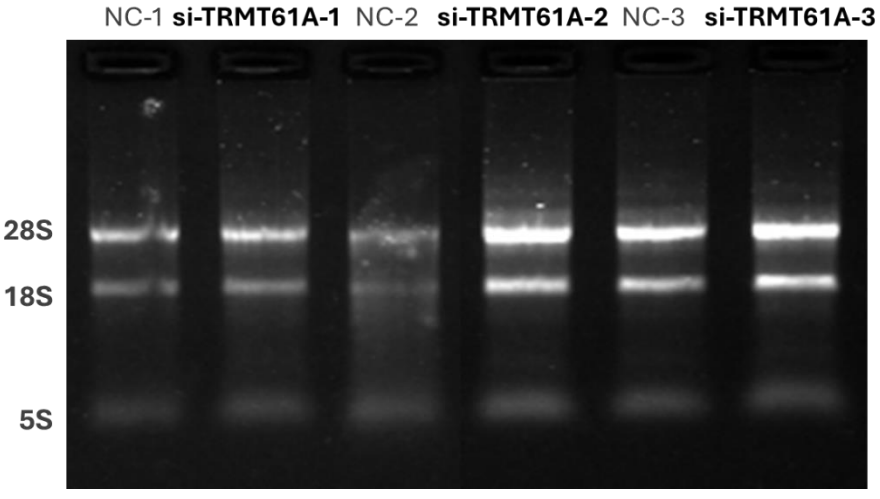


Figure 3.11. The agarose gel image of total RNAs isolated for RNA-Seq from NC and TRMT61A-transfected HCC1143 cells

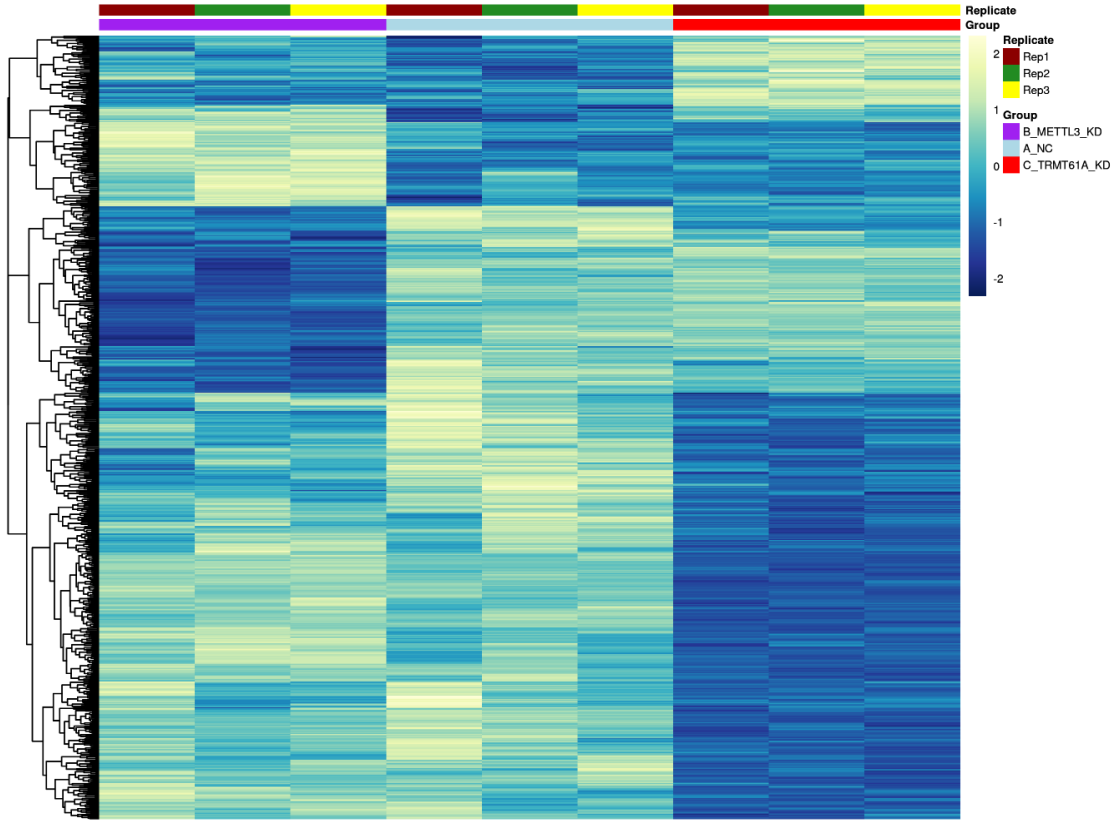


Figure 3.12. Heatmap of differentially expressed genes. Three biological replicates and student's t-test were used for statistical test (1.5-fold greater or smaller).

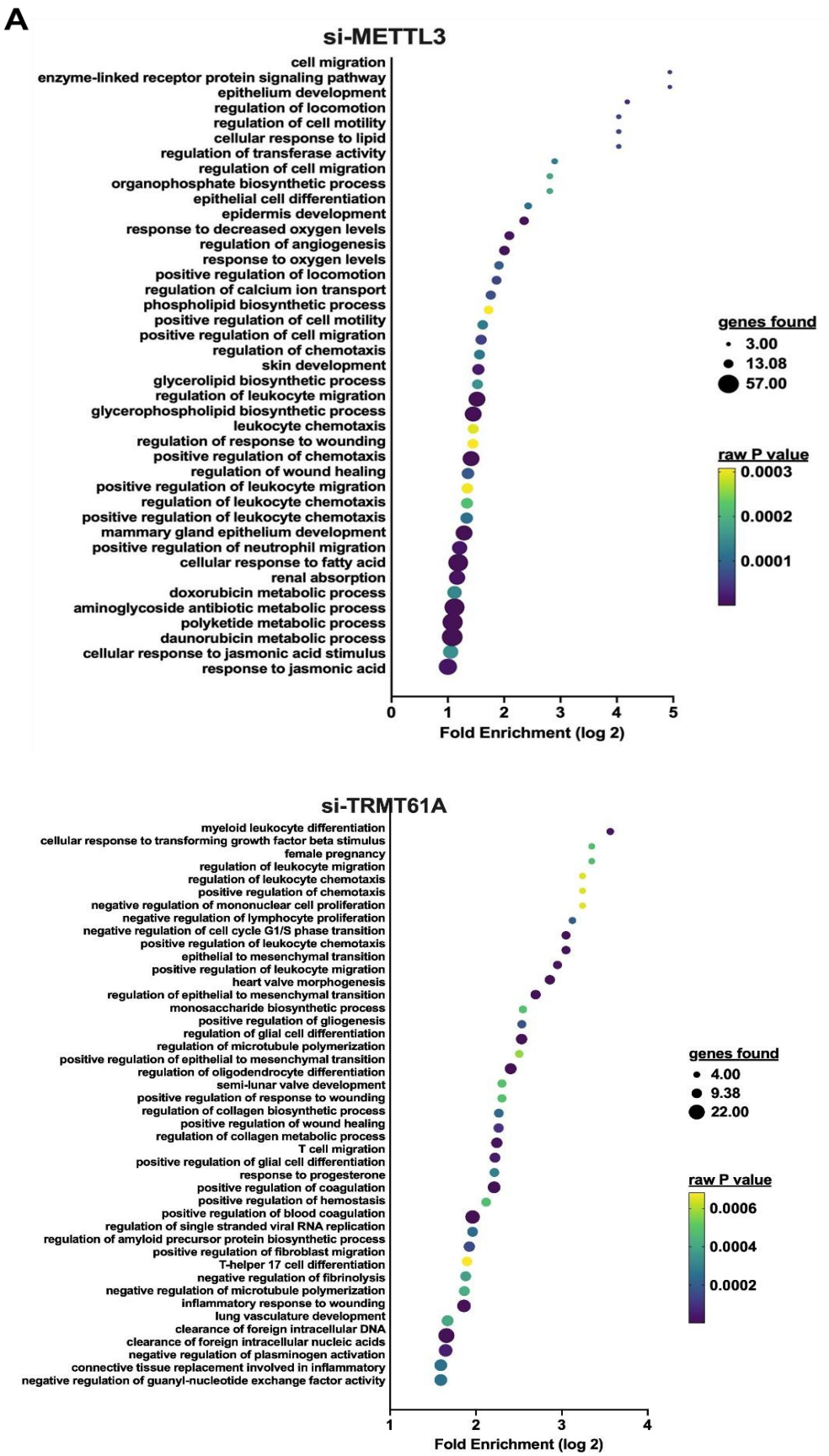


Figure 3.13. GO enrichment analysis of biological pathways for differentially expressed genes in the case of (A) $m^6A$ and (B) $m^1A$ reduction.

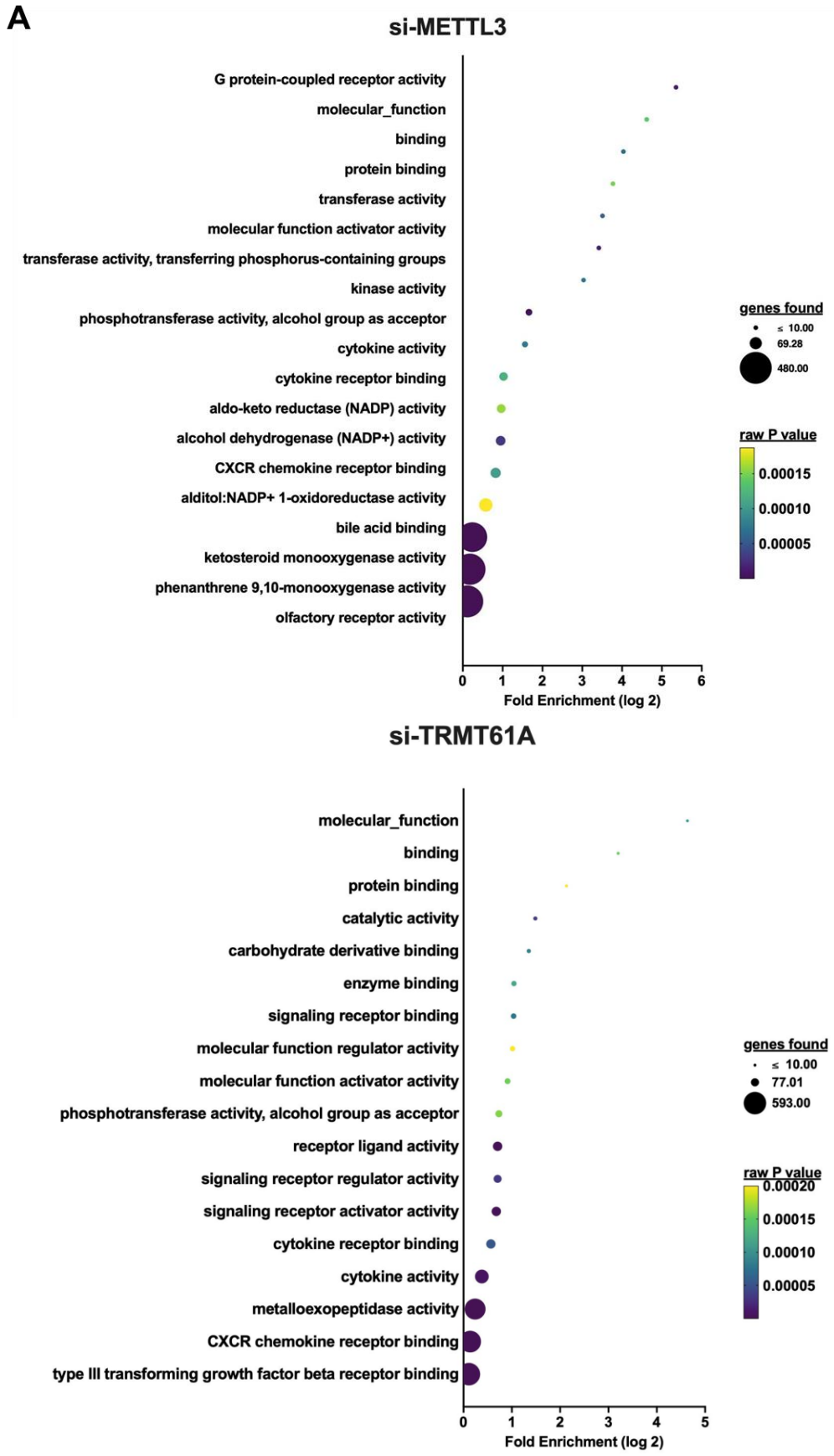


Figure 3.14. GO analysis of molecular function for differentially expressed genes in the case of (A) $m^6A$ and (B) $m^1A$ reduction.

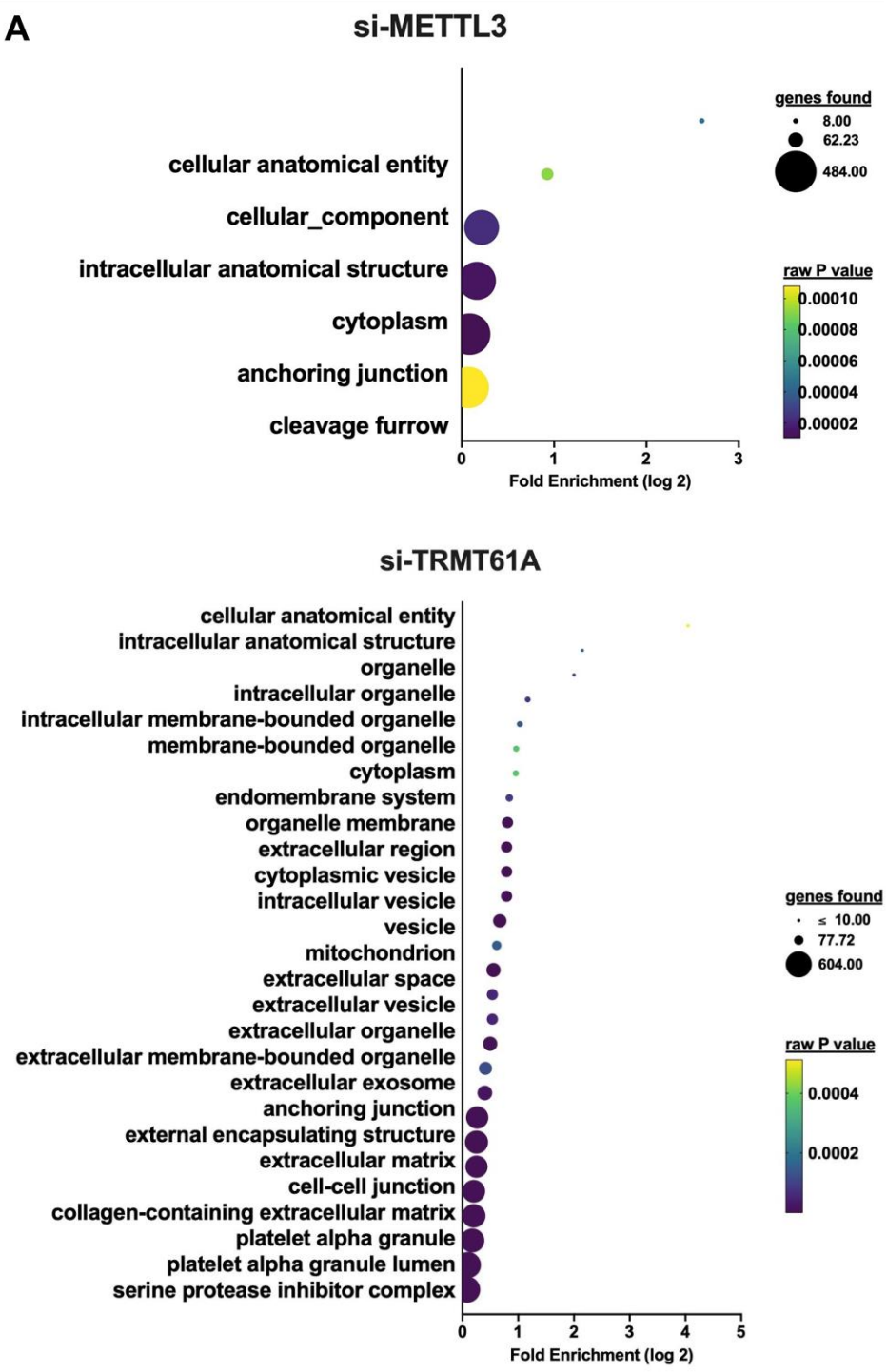


Figure 3.15. GO enrichment analysis of cell component for differentially expressed genes in the case of (A) $m^6A$ and (B) $m^1A$ reduction.

# CHAPTER 4

# DISCUSSION

RNA modifications, which are gaining as much attention as DNA modifications, play various roles in molecular regulations of various cellular phenotypes. $m^6A$ and $m^1A$ methylations, which are located on the adenosine nucleotide and have different regulation mechanisms, are just two of these modifications. These two types of methylation are observed to have different profiles for each type of cancer, based on the proteins in their regulation mechanisms. Even in the subgroups of a cancer type with high rates such as breast cancer, a wide variety of expression levels are observed (Figure 3.1). However, in contrast to $m^6A$ methylation, which is widely studied for its capability of therapeutic function on cancer, $m^1A$ methylation, which is located on the same nucleotide and has common mechanisms such as YTHDF reader proteins, has received less attention (Zou and He 2024; G. Li et al. 2024). In particular, these studies are quite limited in triple-negative breast cancer cells such as HCC1143, one of the most aggressive types of breast cancer. Therefore, this study aimed to determine and compare the phenotypic effects of $m^6A$ and $m^1A$ methylations in HCC1143 cells after knock-down of their writer proteins METTL3 and TRMT61A.

First of all, as shown in Figure 3.3B, it was observed that $m^1A$ writer protein was approximately 2-fold ($P < 0.001$) higher in the HCC1143 cells compared to the healthy cell line MCF10A. When we compared $m^6A$ writer protein level, we found no significant change between HCC1143 and MCF10A cells (Figure 3.3A). Therefore, it was decided to examine the effect of reduction in methylation on mRNA abundance by knocking down the writer proteins of $m^6A$ and $m^1A$, namely METTL3 and TRMT61A, respectively. To determine the maximum level of $m^6A$ reduction, three time points were analyzed after transfection as 48h, 72h and 96h. Knock-down of writer proteins was confirmed by western blot (Figure 3.4) and the decrease of $m^6A$ was determined by a colorimetric $m^6A$ kit. Consequently, the maximum level of reduction of $m^6A$ methylation was achieve at the 72-hour after knock-down of METTL3. The efficiency for METTL3 was 81.8% with a41.2% $m^6A$ reduction while the silencing of TRMT61A was 86.7% for 72h transfection (Figure 3.5). Although there are several methods widely used for genome-wide determination of RNA modifications such as ELISA, miCLIP and SELECT for

methylation detection, there is no practical and cost-friendly technique to determine the total methylation changes that occur in a cell (Anreiter et al. 2021; Zaccara, Ries, and Jaffrey 2019). Therefore, it is important to determine the presence of $m^6A$ by a practical technique such as FTIR Spectroscopy on cellular total RNAs. The results of FTIR spectroscopy measurements show that $m^6A$ methylation changes after si-METTL3 transfection in HCC1143 cells (Figure 3.6). In case of METTL3 silencing in HCC1143, the decrease in the amount of $m^6A$ can be observed by comparing the $CH_3$ peak absorbance value at 2952 $cm^{-1}$ with the $CH_2$ peak absorbance value at 2925 $cm^{-1}$. These differences can also be observed in the symmetric stretching and asymmetric bending regions of $CH_3$ and $CH_2$. The peak absorbance difference value between $CH_3$ and $CH_2$ of METTL3-silenced HCC1143 RNA is higher than the peak difference value between $CH_3$ and $CH_2$ of si-NC. Therefore, this situation occurs due to the decrease in the amount of $m^6A$ in METTL3-silenced HCC1143 RNA (Figure 3.6). In addition, these results led to the ability to detect different RNA modifications, such as m1A, by FTIR.

When the phenotypic effects of these methylations were examined, firstly, the viability of HCC1143 cells was significantly decreased in the case of METTL3 and TRMT61A knock-down (Figure 3.7). Then, the reason of the reduction in proliferation was further interrogated by apoptosis and cell cycle assays. It was interesting that there was no significant change in the apoptosis and arrest of cell cycle check points after reduction of $m^1A$ methylation as shown in Figure 3.8B and 3.9B. However, there was a significant increase in the G2/M check point of cell cycle in the METTL3 knock-down HCC1143 cells (Figure 3.9A). RNA sequencing was performed to examine DEGs upon TRMT61A and METTL3 knockdown, and a heatmap was constructed to highlight the differences between the gene expression patterns upon the knockdown of each writer (Figure 3.12). Apparently, $m^6A$ and $m^1A$ methylations contribute to different pathways as they appear to modulate the abundance of various transcripts (Figure 3.13-15). The number of genes meeting these criteria was 585 in METTL3 silencing, while it was 687 in TRMT61A silencing. Common DEGs were total of 151. In the biological pathway analyses, cell migration, cell motility and enzyme-linked receptor protein signaling were the most significant biological processes (Figure 3.13A). It was demonstrated that $m^6A$ presence has different effects on the cell proliferation and migration based on the stage of breast cancer (Dorgham et al., 2023). However, immune related biological processes and negative regulation of proliferation biological processes were strikingly observed in si-TRMT61A-transfected cells (Figure 3.13B). Currently, various studies are being

carried out to gain insight into the effect of $m^1A$ marks on T cell function (Lin et al., 2023). The effect of $m^1A$ on proliferation of cancer cells has also been reported in various cancer types (Y. Wu et al., 2024). However, it is very important to validate the RNA-seq results by qPCR to reach more conclusive results.

# CHAPTER 5

# CONCLUSION

In this study, the effects and comparison of $m^6A$ and $m^1A$ RNA methylations in HCC1143-triple negative breast cancer cells were validated after knock-down of writer proteins METTL3 and TRMT61A.

When METTL3 and TRMT61A proteins were examined at the protein level in healthy and triple negative cancer cells, although no significant difference was observed in the METTL3 protein, a 2-fold increase in the TRMT61A protein level was observed in HCC1143 cells. After transfection, the highest decrease in the amount of $m^6A$, 41.2%, was observed at 72h. This change in the amount of $m^6A$ was also observed by FTIR spectroscopy, which we showed can be used for total amount of $m^6A$ methylation detection of total RNA. After transfection of 72h METTL3 and TRMT61A writer proteins, a significant decrease in the viability of HCC1143 cells was observed. While no apoptotic changes were observed in either writer protein after their knock-down, a significant increase in the G2/M phase was observed in cell cycle analyzes after METTL3 knock-down. RNA sequencing was performed to examine this phenotypic change from a molecular perspective. As a result of the analyses, it was determined that $m^6A$ and $m^1A$ methylations affected different pathways in HCC1143 triple negative breast cancer cells, as expected. When DEGs with fold change above 1.5 and below -1.5 were evaluated, 585 genes were observed as differentially expressed after $m^6A$ decrease as 41.2% and 687 genes were observed as differentially expressed after $m^1A$ decrease. 151 of the DEGs were common among si-METTL3 and si-TRMT61A HCC1143 cells compared to si-NC HCC1143 cells in the RNA-Seq results. In conclusion, according to the GO enrichment analyses performed with the DEGs obtained; cell motility, migration and enzyme-linked receptor protein signaling pathways were intensely observed after METTL3 knock-down while immune related and negative regulation of proliferation pathways were observed after TRMT61A knock-down.

# REFERENCES


Akçaöz-Alasar, A., Tüncel, Ö., Sağlam, B., Gazaloğlu, Y., Atbinek, M., Cagiral, U., Iscan, E., Ozhan, G., & Akgül, B. (2024). Epitranscriptomics m6A analyses reveal distinct m6A marks under tumor necrosis factor α (TNF-α)-induced apoptotic conditions in HeLa cells. *Journal of Cellular Physiology*, *239*(4). https://doi.org/10.1002/jcp.31176

Alasar, A. A., Tüncel, Ö., Gelmez, A. B., Sağlam, B., Vatansever, İ. E., & Akgül, B. (2022). Genomewide m6A Mapping Uncovers Dynamic Changes in the m6A Epitranscriptome of Cisplatin-Treated Apoptotic HeLa Cells. *Cells*, *11*(23). https://doi.org/10.3390/cells11233905

Anreiter, I., Mir, Q., Simpson, J. T., Janga, S. C., & Soller, M. (2021). New Twists in Detecting mRNA Modification Dynamics. In *Trends in Biotechnology* (Vol. 39, Issue 1, pp. 72–89). Elsevier Ltd. https://doi.org/10.1016/j.tibtech.2020.06.002

Bennett, R. L., & Licht, J. D. (2018). Targeting Epigenetics in Cancer. *Annual Review of Pharmacology and Toxicology Annu. Rev. Pharmacol. Toxicol*, *58*, 187–207. https://doi.org/10.1146/annurev-pharmtox

Berlivet, S., Scutenaire, J., Deragon, J. M., & Bousquet-Antonelli, C. (2019). Readers of the m 6 A epitranscriptomic code. In *Biochimica et Biophysica Acta - Gene Regulatory Mechanisms* (Vol. 1862, Issue 3, pp. 329–342). Elsevier B.V. https://doi.org/10.1016/j.bbagrm.2018.12.008

Bombonati, A., & Sgroi, D. C. (2011). The molecular pathology of breast cancer progression. In *Journal of Pathology* (Vol. 223, Issue 2, pp. 308–318). John Wiley and Sons Ltd. https://doi.org/10.1002/path.2808

Chang, G., Shi, L., Ye, Y., Shi, H., Zeng, L., Tiwary, S., Huse, J. T., Huo, L., Ma, L., Ma, Y., Zhang, S., Zhu, J., Xie, V., Li, P., Han, L., He, C., & Huang, S. (2020). YTHDF3 Induces the Translation of m6A-Enriched Gene Transcripts to Promote Breast

Cancer Brain Metastasis. *Cancer Cell*, *38*(6), 857-871.e7. https://doi.org/10.1016/j.ccell.2020.10.004

Chen, Z., Huang, L., Wang, K., Zhang, L., Zhong, X., Yan, Z., Liu, B., & Zhu, P. (2022). rtcisE2F promotes the self-renewal and metastasis of liver tumor-initiating cells via N 6-methyladenosine-dependent E2F3/E2F6 mRNA stability. *Science China Life Sciences*, *65*(9), 1840–1854. https://doi.org/10.1007/s11427-021-2038-5

Chen, Z., Qi, M., Shen, B., Luo, G., Wu, Y., Li, J., Lu, Z., Zheng, Z., Dai, Q., & Wang, H. (2019). Transfer RNA demethylase ALKBH3 promotes cancer progression via induction of tRNA-derived small RNAs. *Nucleic Acids Research*, *47*(5), 2533–2545. https://doi.org/10.1093/nar/gky1250

Cohn, W. E. (1960). Pseudouridine, a Carbon-Carbon Linked Ribonucleoside in Ribonucleic Acids: Isolation, Structure, and Cehmical Characteristics. *The Journal of Biological Chemistry*, *235*(5), 1488–1498.

Danaei, Hoorn, Lopez, Murray, & Ezzati. (2005). Causes of cancer in the world: comparative risk assessment of nine behavioural and environmental risk factors. *Lancet*, *366*, 1784–1793. http://www.who.int/

Desrosiers, R., Friderici, K., & Rottman, F. (1974). *Identification of Methylated Nucleosides in Messenger RNA from Novikoff Hepatoma Cells (RNA methylation/RNA processing/methylnucleoside composition)* (Vol. 71, Issue 10). https://www.pnas.org

Di Leone, FRAGOMENI, SCARDINA, IONTA, MULE, MAGNO, & TERRIBILE. (2021). Androgen receptor expression and outcome of neoadjuvant chemotherapy in triple-negative breast cancer. *European Review for Medical and Pharmacological Sciences*, *25*, 1910–1915.

Dominissini, D., Moshitch-Moshkovitz, S., Schwartz, S., Salmon-Divon, M., Ungar, L., Osenberg, S., Cesarkas, K., Jacob-Hirsch, J., Amariglio, N., Kupiec, M., Sorek, R., & Rechavi, G. (2012). Topology of the human and mouse m6A RNA methylomes

revealed by m6A-seq. *Nature*, *485*(7397), 201–206. https://doi.org/10.1038/nature11112

Dominissini, D., Nachtergaele, S., Moshitch-Moshkovitz, S., Peer, E., Kol, N., Ben-Haim, M. S., Dai, Q., Di Segni, A., Salmon-Divon, M., Clark, W. C., Zheng, G., Pan, T., Solomon, O., Eyal, E., Hershkovitz, V., Han, D., Doré, L. C., Amariglio, N., Rechavi, G., & He, C. (2016). The dynamic N1 -methyladenosine methylome in eukaryotic messenger RNA. *Nature*, *530*(7591), 441–446. https://doi.org/10.1038/nature16998

Dorgham, M. G., Elliott, B. A., Holley, C. L., & Mansfield, K. D. (2023). m6A regulates breast cancer proliferation and migration through stage-dependent changes in Epithelial to Mesenchymal Transition gene expression. *Frontiers in Oncology*, *13*. https://doi.org/10.3389/fonc.2023.1268977

Duan, M., Liu, H., Xu, S., Yang, Z., Zhang, F., Wang, G., Wang, Y., Zhao, S., & Jiang, X. (2024). IGF2BPs as novel m6A readers: Diverse roles in regulating cancer cell biological functions, hypoxia adaptation, metabolism, and immunosuppressive tumor microenvironment. In *Genes and Diseases* (Vol. 11, Issue 2, pp. 890–920). KeAi Communications Co. https://doi.org/10.1016/j.gendis.2023.06.017

El Yacoubi, B., Bailly, M., & De Crécy-Lagard, V. (2012). Biosynthesis and function of posttranscriptional modifications of transfer RNAs. *Annual Review of Genetics*, *46*, 69–95. https://doi.org/10.1146/annurev-genet-110711-155641

Engel, M., Eggert, C., Kaplick, P. M., Eder, M., Röh, S., Tietze, L., Namendorf, C., Arloth, J., Weber, P., Rex-Haffner, M., Geula, S., Jakovcevski, M., Hanna, J. H., Leshkowitz, D., Uhr, M., Wotjak, C. T., Schmidt, M. V., Deussing, J. M., Binder, E. B., & Chen, A. (2018). The Role of m6A/m-RNA Methylation in Stress Response Regulation. *Neuron*, *99*(2), 389-403.e9. https://doi.org/10.1016/j.neuron.2018.07.009

Esteller, M., & Pandolfi, P. P. (2017). The epitranscriptome of noncoding RNAs in cancer. *Cancer Discovery*, *7*(4), 359–368. https://doi.org/10.1158/2159-8290.CD-16-1292

Esteva-Socias, M., & Aguilo, F. (2024). METTL3 as a master regulator of translation in cancer: mechanisms and implications. *NAR Cancer*, *6*(1). https://doi.org/10.1093/narcan/zcae009

Fang, Z., Mei, W., Qu, C., Lu, J., Shang, L., Cao, F., & Li, F. (2022). Role of m6A writers, erasers and readers in cancer. In *Experimental Hematology and Oncology* (Vol. 11, Issue 1). BioMed Central Ltd. https://doi.org/10.1186/s40164-022-00298-7

Garcias Morales, D., & Reyes, J. L. (2021). A birds'-eye view of the activity and specificity of the mRNA m6A methyltransferase complex. In *Wiley Interdisciplinary Reviews: RNA* (Vol. 12, Issue 1). Blackwell Publishing Ltd. https://doi.org/10.1002/wrna.1618

Harbeck, N., Penault-Llorca, F., Cortes, J., Gnant, M., Houssami, N., Poortmans, P., Ruddy, K., Tsang, J., & Cardoso, F. (2019). Breast cancer. *Nature Reviews Disease Primers*, *5*(1). https://doi.org/10.1038/s41572-019-0111-2

He, L., Li, H., Wu, A., Peng, Y., Shu, G., & Yin, G. (2019). Functions of N6-methyladenosine and its role in cancer. In *Molecular Cancer* (Vol. 18, Issue 1). BioMed Central Ltd. https://doi.org/10.1186/s12943-019-1109-9

Hotchkiss, R. D. (1948). *THE QUANTITATIVE SEPARATION OF PURINES, PYRIMIDINES, AND NUCLEOSIDES BY PAPER CHROMATOGRAPHY*.

Jia, G., Yang, C. G., Yang, S., Jian, X., Yi, C., Zhou, Z., & He, C. (2008). Oxidative demethylation of 3-methylthymine and 3-methyluracil in single-stranded DNA and RNA by mouse and human FTO. *FEBS Letters*, *582*(23–24), 3313–3319. https://doi.org/10.1016/j.febslet.2008.08.019

Jin, Y., Liu, P., Chaoyang, B., Liu, J., Wang, Y., Ren, W., Tang, X., Shi, X., Pan, D., Tian, G., & Yang, L. (2023). *Effect of m 1 A regulators on prognosis of colorectal cancer*. https://doi.org/10.21203/rs.3.rs-2735472/v1

Jonkhout, N., Tran, J., Smith, M. A., Schonrock, N., Mattick, J. S., & Novoa, E. M. (2017). *The RNA modification landscape in human disease*. https://doi.org/10.1261/rna.063503

Kamiloglu, S., Sari, G., Ozdal, T., & Capanoglu, E. (2020). Guidelines for cell viability assays. *Food Frontiers*, *1*(3), 332–349. https://doi.org/10.1002/fft2.44

Kumari, K., Groza, P., & Aguilo, F. (2021). Regulatory roles of RNA modifications in breast cancer. In *NAR Cancer* (Vol. 3, Issue 3). Oxford University Press. https://doi.org/10.1093/narcan/zcab036

Lee, J. (2023). Current Treatment Landscape for Early Triple-Negative Breast Cancer (TNBC). In *Journal of Clinical Medicine* (Vol. 12, Issue 4). MDPI. https://doi.org/10.3390/jcm12041524

Li, G., Yao, Q., Liu, P., Zhang, H., Liu, Y., Li, S., Shi, Y., Li, Z., & Zhu, W. (2024). Critical roles and clinical perspectives of RNA methylation in cancer. In *MedComm* (Vol. 5, Issue 5). John Wiley and Sons Inc. https://doi.org/10.1002/mco2.559

Li, X., Xiong, X., Zhang, M., Wang, K., Chen, Y., Zhou, J., Mao, Y., Lv, J., Yi, D., Chen, X. W., Wang, C., Qian, S. B., & Yi, C. (2017). Base-Resolution Mapping Reveals Distinct m1A Methylome in Nuclear- and Mitochondrial-Encoded Transcripts. *Molecular Cell*, *68*(5), 993-1005.e9. https://doi.org/10.1016/j.molcel.2017.10.019

Lin, P., Li, G., & Wu, M. (2023). RNA methylation into m1A era: a new regulation over T-cell function. *Signal Transduction and Targeted Therapy*, *8*(1), 78. https://doi.org/10.1038/s41392-023-01360-4

Liu, Y., Zhang, S., Gao, X., Ru, Y., Gu, X., & Hu, X. (2024a). Research progress of N1-methyladenosine RNA modification in cancer. In *Cell Communication and Signaling* (Vol. 22, Issue 1). BioMed Central Ltd. https://doi.org/10.1186/s12964-023-01401-z

Liu, Y., Zhang, S., Gao, X., Ru, Y., Gu, X., & Hu, X. (2024b). Research progress of N1-methyladenosine RNA modification in cancer. In *Cell Communication and Signaling* (Vol. 22, Issue 1). BioMed Central Ltd. https://doi.org/10.1186/s12964-023-01401-z

Motorin, Y., & Helm, M. (2011). RNA nucleotide methylation. In *Wiley Interdisciplinary Reviews: RNA* (Vol. 2, Issue 5, pp. 611–631). https://doi.org/10.1002/wrna.79

Nik-Zainal, S., Davies, H., Staaf, J., Ramakrishna, M., Glodzik, D., Zou, X., Martincorena, I., Alexandrov, L. B., Martin, S., Wedge, D. C., Van Loo, P., Ju, Y. S., Smid, M., Brinkman, A. B., Morganella, S., Aure, M. R., Lingjærde, O. C., Langerød, A., Ringnér, M., … Stratton, M. R. (2016). Landscape of somatic mutations in 560 breast cancer whole-genome sequences. *Nature*, *534*(7605), 47–54. https://doi.org/10.1038/nature17676

Niu, Y., Lin, Z., Wan, A., Chen, H., Liang, H., Sun, L., Wang, Y., Li, X., Xiong, X. F., Wei, B., Wu, X., & Wan, G. (2019). RNA N6-methyladenosine demethylase FTO promotes breast tumor progression through inhibiting BNIP3. *Molecular Cancer*, *18*(1). https://doi.org/10.1186/s12943-019-1004-4

Patil, D. P., Chen, C. K., Pickering, B. F., Chow, A., Jackson, C., Guttman, M., & Jaffrey, S. R. (2016). M6 A RNA methylation promotes XIST-mediated transcriptional repression. *Nature*, *537*(7620), 369–373. https://doi.org/10.1038/nature19342

Pommerenke, C., Nagel, S., Haake, J., Koelz, A. L., Christgen, M., Steenpass, L., & Eberth, S. (2024). Molecular Characterization and Subtyping of Breast Cancer Cell Lines Provide Novel Insights into Cancer Relevant Genes. *Cells*, *13*(4). https://doi.org/10.3390/cells13040301

Pozarowski, P., & Darzynkiewicz, Z. (2004). Analysis of Cell Cycle by Flow Cytometry. *In: Schönthal, A.H. (Eds) Checkpoint Controls and Cancer. Methods in Molecular Biology*, *281*, 301–311.

Qian, J. Y., Gao, J., Sun, X., Cao, M. Da, Shi, L., Xia, T. S., Zhou, W. Bin, Wang, S., Ding, Q., & Wei, J. F. (2019). KIAA1429 acts as an oncogenic factor in breast cancer by regulating CDK1 in an N6-methyladenosine-independent manner. *Oncogene*, *38*(33), 6123–6141. https://doi.org/10.1038/s41388-019-0861-z

Qiao, Y., Sun, Q., Chen, X., He, L., Wang, D., Su, R., Xue, Y., Sun, H., & Wang, H. (2023). Nuclear m6A Reader YTHDC1 Promotes Muscle Stem Cell Activation/Proliferation by Regulating mRNA Splicing and Nuclear Export. *ELife*, *12*. https://doi.org/10.7554/elife.82703

Ries, R. J., Zaccara, S., Klein, P., Olarerin-George, A., Namkoong, S., Pickering, B. F., Patil, D. P., Kwak, H., Lee, J. H., & Jaffrey, S. R. (2019). m6A enhances the phase separation potential of mRNA. *Nature*, *571*(7765), 424–428. https://doi.org/10.1038/s41586-019-1374-1

Roundtree, I. A., Evans, M. E., Pan, T., & He, C. (2017). Dynamic RNA Modifications in Gene Expression Regulation. In *Cell* (Vol. 169, Issue 7, pp. 1187–1200). Cell Press. https://doi.org/10.1016/j.cell.2017.05.045

Sadida, H. Q., Abdulla, A., Marzooqi, S. Al, Hashem, S., Macha, M. A., Akil, A. S. A. S., & Bhat, A. A. (2024). Epigenetic modifications: Key players in cancer heterogeneity and drug resistance. *Translational Oncology*, *39*. https://doi.org/10.1016/j.tranon.2023.101821

Sağlam, B., & Akgül, B. (2024a). An Overview of Current Detection Methods for RNA Methylation. In *International Journal of Molecular Sciences* (Vol. 25, Issue 6). Multidisciplinary Digital Publishing Institute (MDPI). https://doi.org/10.3390/ijms25063098

Sağlam, B., & Akgül, B. (2024b). An Overview of Current Detection Methods for RNA Methylation. In *International Journal of Molecular Sciences* (Vol. 25, Issue 6). Multidisciplinary Digital Publishing Institute (MDPI). https://doi.org/10.3390/ijms25063098

Sharma, S., Watzinger, P., Kötter, P., & Entian, K. D. (2013). Identification of a novel methyltransferase, Bmt2, responsible for the N-1-methyl-adenosine base modification of 25S rRNA in Saccharomyces cerevisiae. *Nucleic Acids Research*, *41*(10), 5428–5443. https://doi.org/10.1093/nar/gkt195

Shi, H., Wang, X., Lu, Z., Zhao, B. S., Ma, H., Hsu, P. J., Liu, C., & He, C. (2017). YTHDF3 facilitates translation and decay of N 6-methyladenosine-modified RNA. *Cell Research*, *27*(3), 315–328. https://doi.org/10.1038/cr.2017.15

Starr, J. L., & Sells, B. H. (1969). *Methylated Ribonucleic Acids*. www.physiology.org/journal/physrev

Taylor, R. A., Fraser, M., Rebello, R. J., Boutros, P. C., Murphy, D. G., Bristow, R. G., & Risbridger, G. P. (2019). The influence of BRCA2 mutation on localized prostate cancer. In *Nature Reviews Urology* (Vol. 16, Issue 5, pp. 281–290). Nature Publishing Group. https://doi.org/10.1038/s41585-019-0164-8

Wang, H., Xu, B., & Shi, J. (2020). N6-methyladenosine METTL3 promotes the breast cancer progression via targeting Bcl-2. *Gene*, *722*. https://doi.org/10.1016/j.gene.2019.144076

Wang, J. yan, & Lu, A. qing. (2021). The biological function of m6A reader YTHDF2 and its role in human disease. In *Cancer Cell International* (Vol. 21, Issue 1). BioMed Central Ltd. https://doi.org/10.1186/s12935-021-01807-0

Wei, C.-M., Gershowitz, A., & Moss, B. (1975). Methylated Nucleotides Block 5’ Terminus of HeLa Cell Messenger RNA. In *Cell* (Vol. 4).

Wojtas, M. N., Pandey, R. R., Mendel, M., Homolka, D., Sachidanandam, R., & Pillai, R. S. (2017). Regulation of m6A Transcripts by the 3′→5′ RNA Helicase YTHDC2 Is Essential for a Successful Meiotic Program in the Mammalian Germline. *Molecular Cell*, *68*(2), 374-387.e12. https://doi.org/10.1016/j.molcel.2017.09.021

Woo, H. H., & Chambers, S. K. (2019). Human ALKBH3-induced m1A demethylation increases the CSF-1 mRNA stability in breast and ovarian cancer cells. *Biochimica et Biophysica Acta - Gene Regulatory Mechanisms*, *1862*(1), 35–46. https://doi.org/10.1016/j.bbagrm.2018.10.008

Wu, H., & Yi, E. S. (2006). Epigenetic regulation of stem cell differentiation. In *Pediatric Research* (Vol. 59, Issue 4 PART. 2). https://doi.org/10.1203/01.pdr.0000203565.76028.2a

Wu, L., Wu, D., Ning, J., Liu, W., & Zhang, D. (2019). Changes of N6-methyladenosine modulators promote breast cancer progression. *BMC Cancer*, *19*(1). https://doi.org/10.1186/s12885-019-5538-z

Wu, Y., Chen, Z., & Xie, G. (2024). *RNA m1A methylation regulates glycolysis of cancer cells through modulating ATP5D*. https://doi.org/10.1073/pnas

Zaccara, S., Ries, R. J., & Jaffrey, S. R. (2019). Reading, writing and erasing mRNA methylation. In *Nature Reviews Molecular Cell Biology* (Vol. 20, Issue 10, pp. 608–624). Nature Publishing Group. https://doi.org/10.1038/s41580-019-0168-5

Zhang, C., & Jia, G. (2018). Reversible RNA Modification N1-methyladenosine (m1A) in mRNA and tRNA. In *Genomics, Proteomics and Bioinformatics* (Vol. 16, Issue 3, pp. 155–161). Beijing Genomics Institute. https://doi.org/10.1016/j.gpb.2018.03.003

Zhao, F., Xu, Y., Gao, S., Qin, L., Austria, Q., Siedlak, S. L., Pajdzik, K., Dai, Q., He, C., Wang, W., O'Donnell, J. M., Tang, B., & Zhu, X. (2021). METTL3-dependent RNA m6A dysregulation contributes to neurodegeneration in Alzheimer's disease through aberrant cell cycle events. *Molecular Neurodegeneration*, *16*(1). https://doi.org/10.1186/s13024-021-00484-x

Zheng, G., Dahl, J. A., Niu, Y., Fedorcsak, P., Huang, C. M., Li, C. J., Vågbø, C. B., Shi, Y., Wang, W. L., Song, S. H., Lu, Z., Bosmans, R. P. G., Dai, Q., Hao, Y. J., Yang, X., Zhao, W. M., Tong, W. M., Wang, X. J., Bogdan, F., … He, C. (2013). ALKBH5 Is a Mammalian RNA Demethylase that Impacts RNA Metabolism and Mouse Fertility. *Molecular Cell*, *49*(1), 18–29. https://doi.org/10.1016/j.molcel.2012.10.015

Zong, X., Xiao, X., Shen, B., Jiang, Q., Wang, H., Lu, Z., Wang, F., Jin, M., Min, J., Wang, F., & Wang, Y. (2021). The N6-methyladenosine RNA-binding protein YTHDF1 modulates the translation of TRAF6 to mediate the intestinal immune response. *Nucleic Acids Research*, *49*(10), 5537–5552. https://doi.org/10.1093/nar/gkab343

Zou, Z., & He, C. (2024). The YTHDF proteins display distinct cellular functions on m6A-modified RNA. In *Trends in Biochemical Sciences*. Elsevier Ltd. https://doi.org/10.1016/j.tibs.2024.04.001